Heliyon 10 (2024) e39301

Contents lists available at ScienceDirect

Heliyon

journal homepage: www.cell.com/heliyon

Research article

Multi-strategy improved runge kutta optimizer and its promise to estimate the model parameters of solar photovoltaic modules

Serdar Ekinci [a,*], Rizk M. Rizk-Allah [b], Davut Izci [a,c,d], Emre Çelik [e]

[a] Department of Computer Engineering, Batman University, Batman, 72100, Turkey
[b] Basic Engineering Science Department, Faculty of Engineering, Menoufia University, Shebin El-Kom, 32511, Egypt
[c] Applied Science Research Center, Applied Science Private University, Amman, 11931, Jordan
[d] MEU Research Unit, Middle East University, Amman, 11831, Jordan
[e] Department of Electrical and Electronics Engineering, Düzce University, Düzce, Turkey

ARTICLE INFO

Keywords:
Improved Runge Kutta (RUN) optimizer
Solar photovoltaic (PV) unit
I-V characteristic
Parameter estimation
Single and double diode models

ABSTRACT

Harnessing the potential of solar photovoltaic (PV) technology relies heavily on accurately estimating the model parameters of PV cells/modules using real current-voltage (I-V) data. Achieving optimal parameter values is essential for the performance and efficiency of PV systems, necessitating the use of advanced optimization techniques. In our endeavor, we introduce a multi-strategy improvement approach for the Runge Kutta (RUN) optimizer, a cutting-edge tool used for tackling this critical task in both single-diode and double-diode PV unit models. By aligning experimental and model-based estimated data, our approach seeks to reduce errors and improve the accuracy of PV system performance. We conduct meticulous analyses of two compelling case studies and the CEC 2020 test suite to showcase the versatility and effectiveness of our improved RUN (IRUN) algorithm. The first case study involves a standard dataset derived from the well-known R.T.C. France silicon solar cell, where IRUN performs favorably compared to competing methods, demonstrating its effectiveness. IRUN effectively manages the complex task of defining model parameters for an industrial PV module situated at the Engineering Faculty of Düzce University in Turkey. The real-world I-V data, obtained under optimal conditions with a temperature of $30^{\circ}C$ and solar radiance of $1000W/m^2$, provide strong evidence of the practical applicability and real-world benefits of our innovative method. Additional analyses through three-diode and PV module models further confirm the efficacy of the IRUN. A mean absolute error of down to 6.5E-04 and root mean square error of down to 7.3668E-04 are achieved. Our approach provides a practical and efficient tool for improving the accuracy of PV systems, enhancing their performance when compared to existing methods.

1. Introduction

In recent years, researchers have turned their attention to renewable energy sources, which have become a dynamic and ever-evolving field. In today's world, where we grapple with the urgent issues of global warming, sustainability has become a top priority [1]. Solar energy, often hailed as the future of energy, offers hope because it's eco-friendly. As we deal with the dwindling supply of

* Corresponding author.
E-mail addresses: ekinciser@yahoo.com, serdar.ekinci@batman.edu.tr (S. Ekinci), rizk_masoud@yahoo.com (R.M. Rizk-Allah), davutizci@gmail.com, davut.izci@batman.edu.tr (D. Izci), emrecelik@duzce.edu.tr (E. Çelik).

https://doi.org/10.1016/j.heliyon.2024.e39301
Received 22 May 2023; Received in revised form 2 October 2024; Accepted 10 October 2024
Available online 12 October 2024
2405-8440/© 2024 The Authors. Published by Elsevier Ltd. This is an open access article under the CC BY-NC license (http://creativecommons.org/licenses/by-nc/4.0/).

petroleum, increasing pollution, and the undeniable effects of climate change, solar power emerges as a compelling solution [2,3]. Among the various options for sustainable energy, solar photovoltaic (PV) energy stands out as a clean and accessible choice with reasonable costs for setup and operation. However, the efficiency of PV systems depends on environmental factors like sunlight and temperature. To make PV systems work their best, we need to choose the right models [4,5]. The key to optimizing these models is getting accurate estimates for their parameters. But this is not a straightforward task because PV technology is inherently complex and nonlinear. In response, researchers have come up with many different strategies [6–14].

In understanding the non-linear I-V characteristics of PV systems, two commonly used equivalent circuits have emerged. These circuits are known as the single-diode model (SDM) and the double-diode model (DDM), and they approach the task differently [15]. The SDM is favored for its simplicity and fewer adjustable parameters, providing clear advantages over the DDM [15]. However, the DDM steps in to address the limitations of the SDM by introducing an additional diode to account for recombination losses. In both models, critical parameters like the photo-generated current, parallel/shunt circuit resistance, series resistance, saturation current, and ideality factors play vital roles in defining and shaping the behavior of PV units [16].

In the field of PV modeling, researchers have developed various methods that can be categorized into three main groups: deterministic, analytical, and heuristic. Analytical techniques are based on mathematical analyses, which offer the advantage of faster and simpler calculations. However, they often sacrifice precision and consistency, which can affect the reliability of the results [17]. Deterministic approaches provide solutions but have limitations because they rely on models that require differentiation and convexity. Heuristic approaches, on the other hand, offer a way to overcome these limitations. They have a remarkable ability to handle complex problems with multiple objectives and address the challenges at hand [18]. This is why metaheuristic optimization methods have become widely accepted as a solution for dealing with the complexities of parameter identification in solar PV systems [19].

In the quest for precise modeling of solar PV systems, researchers have introduced various optimization algorithms. These algorithms fall into different categories, each with its strengths and weaknesses. For instance, in Ref. [20], researchers reported an efficient and accurate gradient-based optimizer for extracting parameters from solar cells and PV modules. In Ref. [21], an improved optimization algorithm was developed, combining a gradient-based optimizer with a chaotic sequence generator to estimate PV parameters for solar cells and modules. They evaluated the effectiveness of this hybrid algorithm using diverse datasets from various solar cells and modules. Another approach, the improved moth-flame algorithm introduced in Ref. [22], enhanced precision and efficiency compared to its original version, albeit at the cost of increased computation time. In Ref. [23], the musical chairs algorithm was used to speed up and improve the accuracy of PV parameter estimation by involving multiple search agents to enhance exploration and reduce convergence times. In Ref. [24], researchers explored a novel hybrid mechanism combining wild horse and hunter-prey models to determine PV characteristics. This hybrid mechanism's effectiveness was validated through case studies involving R.T.C. France silicon solar cells, Photowatt-PWP201 panels, and thin-film PV systems under varying conditions. While [25] utilized the continuous population genetic algorithm to estimate parameters from experimental datasets of PV units, limited success was attributed to solely relying on the SDM technique and four specific panel types. In Ref. [26], the modified salp swarm algorithm was proposed to identify parameters for PV models, specifically the SDM and DDM. The modifications in the salp swarm algorithm addressed early convergence issues and improved exploration potential, although reducing the root mean square error (RMSE) value remained challenging. While several approaches for modeling solar PV cells/modules have been explored in the literature [27–34], there's still room for more effective optimization algorithms to achieve superior results.

Considering the challenges mentioned earlier and the promising potential of metaheuristic methods, this paper aims to introduce an innovative metaheuristic algorithm for accurately estimating parameters in PV systems. We achieve this by enhancing the recently developed Runge-Kutta optimizer [35] with a set of ingenious improvements. We utilize a quadratic interpolation strategy, a Laplacian segment mutation technique, a Levy flight strategy, and information-sharing-based local search mechanisms to significantly improve the accuracy and efficiency of PV system parameter estimation. This paper presents a groundbreaking approach by leveraging an improved version of the Runge-Kutta optimizer to precisely determine optimal combinations of solar PV parameters in the context of SDM, DDM, three-diode model (TDM) and PV module models. Our primary goal is to identify parameter values that minimize the differences between measured and estimated I-V data, enhancing the precision of PV system characterization. To demonstrate the strength of our proposal, we conduct a comprehensive analysis using CEC 2020 benchmark functions and two compelling case studies: the R.T.C. France silicon solar cell dataset and data collected from the CS6P-220P solar module. Besides, we perform the analyses on two additional models, TDM of R.TC. France silicon solar cell and PV model of STM6-40/36 PV module.

We initially evaluated the performance of our proposed algorithm using the CEC 2020 benchmark test suite and compared it to several other optimization algorithms, including the dwarf mongoose optimization algorithm [36], salp swarm algorithm [37], grey wolf optimizer [38], prairie dog optimization algorithm [39], biogeography-based optimization [40], particle swarm optimization [41], gazelle optimization algorithm [42], differential evolution [43] and sine cosine algorithm [44]. The results clearly demonstrate that our proposed algorithm consistently outperforms the others, achieving the best average values for all CEC 2020 benchmark functions. This demonstrates its strong performance.

In PV system analysis, we use a well-recognized dataset from R.T.C. France, involving silicon solar cells. We employ the improved Runge-Kutta optimizer to enhance the accuracy and efficiency of optimizing the SDM and DDM parameters of these cells. This optimization process is marked by unparalleled precision and effectiveness. To emphasize the novelty and significance of our work, we conduct a thorough comparison against the latest advancements in optimization algorithms, including the squirrel search algorithm [15], elite learning adaptive differential evolution [45], hybrid multi-group stochastic cooperative particle swarm optimization [46], queuing search optimization and differential evolution [47], hybrid chaotic northern goshawk and pattern search [48], hybrid chimp algorithm [49], flexible improved particle swarm optimization and sequential quadratic programming [50], weighted mean of vectors algorithm [51], differential evolution [52], sine cosine differential gradient based optimizer [53], quantum Nelder-Mead hunger

games search algorithm [54], improved tunicate swarm algorithm [55], enhanced Harris hawk optimization [56], gradient based optimization with ranking mechanisms [57], stochastic fractal search algorithm [58], coyote optimization algorithm [59], improved Lozi map based chaotic optimization algorithm [60], improved moth-flame optimization [61], hybrid firefly and pattern search algorithm [62], improved jaya optimization algorithm [63], artificial bee colony optimization [64], conscious neighborhood strategy-based Laplacian barnacles mating algorithm [28] and war strategy optimization [32]. Additionally, to replicate real-world conditions, we utilize an experimental dataset from a polycrystalline CS6P-220P solar module. This dataset was collected through rigorous experimentation at the Engineering Faculty of Düzce University in Turkey. Using I-V data from this PV module, the improved Runge-Kutta optimizer refines the SDM and DDM parameters, guided by the RMSE objective function. This process enhances the algorithm's performance, offering significant improvements in PV parameter estimation. The efficacy of the proposed method is also demonstrated through additional analyses on TDM of R.TC. France silicon solar cell and PV model of STM6-40/36 PV module. In line with the above discussion, the novelty and the contributions of our study can be listed as follows.

1. Our study introduces an innovative metaheuristic algorithm that enhances the recently developed Runge-Kutta optimizer with novel techniques, including quadratic interpolation, Laplacian segment mutation, Levy flight, and information-sharing-based local search mechanisms.
2. Our proposed algorithm undergoes comprehensive evaluation, including benchmarking against various state-of-the-art optimization algorithms using the CEC 2020 benchmark test suite.
3. The results of our study demonstrate that our proposed algorithm consistently outperforms other optimization algorithms, achieving the best average values for all CEC 2020 benchmark functions.
4. We further validate our approach using a well-recognized dataset from R.T.C. France silicon solar cells and an experimental dataset from a polycrystalline CS6P-220P solar module, replicating real-world conditions.
5. Our approach enables the precise determination of optimal combinations of solar PV parameters, particularly within the context of the SDM and DDM.
6. We demonstrate the efficiency of our proposed method The performance through additional analyses on TDM and PV models.
7. By improving PV parameter estimation, our research contributes to the advancement of sustainable and efficient solar energy solutions, addressing the pressing challenges of global warming and climate change.

2. Runge Kutta optimizer

The **RUN**ge–Kutta optimization (RUN) algorithm is a new meta-heuristic framework that was purported by Iman Ahmadianfar et al. [35] based on iterative Runge-Kutta (IRK) model. The IRK has been used to find the approximate solutions for the ordinary differential equations (ODEs). In terms of optimization point of view, the algorithm starts with the initial solutions of M agents constructed within the bounds of the search landscape. Accordingly RUN employs two operators for updating purposes which are the Runge-Kutta-based searching mechanism (SM) and solution enhancement operator (SEO). The following subsections exhibit the main procedures of the RUN algorithm.

2.1. Updating solutions

The current solution (Δ_i) at the candidate iteration is updated based on the SM perspective of IRK theory as follows.

$$\Delta_{new1} = \begin{cases} (\Delta_b + r.SF.e.\Delta_b) + SF.SM + \omega.randn.(\Delta_d - \Delta_b) & rand < 0.5 \\ (\Delta_d + r.SF.e.\Delta_d) + SF.SM + \omega.randn.(\Delta_{a1} - \Delta_{a2}) & Otherwise \end{cases} \tag{1}$$

where r stands for an integer with 1 or -1 value, e denotes a random number ranged from 0 to 2, ω denotes a random number; Δ_{a1} and Δ_{a2} are two solutions that are selected at random in the range of $[0, M]$; M denotes the population size; $randn$ defines a random number that generates values based on the normal distribution; SF stands for an adaptive factor that is expressed as follows:

$$SF = 2.(0.5 - rand) \times \delta \tag{2}$$

$$\delta = a \times exp\left(- b \times rand \times \left(\frac{it}{T_{max}}\right)\right) \tag{3}$$

where it and T_{max} denote the present iteration and largest iteration number, respectively. Besides, a and b are control parameters that has default values of 20 and 12, respectively. Further, the Δ_b and Δ_d are represented by:

$$\Delta_b = \varphi \times \Delta_i + (1 - \varphi) \times \Delta_{a1}, i = 1, 2, .., M \tag{4}$$

$$\Delta_d = \varphi \times \Delta_{best} + (1 - \varphi) \times \Delta_{cbest} \tag{5}$$

where φ signifies a random number within the range (0,1), Δ_{best} identifies the best-so-far solution, and Δ_{cbest} represents the best position detected at each iteration. The SM is given by:

$$SM = \frac{1}{6}(\Delta_{IRK}).\Delta x \tag{6}$$

$$\Delta_{IRK} = g_1 + 2.g_2 + 2.g_3 + g_4$$

$$g_1 = \frac{1}{2\Delta x}(rand.\Delta_{ws} - \nu.\Delta_{best})$$

$$\nu = (1 - rand).round(1 + rand)$$

$$g_2 = \frac{1}{2\Delta x}(rand.(\Delta_{ws} + r_1.g_1.\Delta x) - (\nu.\Delta_{best} + r_2.g_1.\Delta x))$$

$$g_3 = \frac{1}{2\Delta x}\left(rand.\left(\Delta_{ws} + r_1.\left(\frac{1}{2}g_2\right).\Delta x\right) - \left(\nu.\Delta_{best} + r_2.\left(\frac{1}{2}g_2\right).\Delta x\right)\right)$$

$$g_4 = \frac{1}{2\Delta x}(rand.(\Delta_{ws} + r_1.g_3.\Delta x) - (\nu.\Delta_{best} + r_2.g_3.\Delta x))$$

where Δ_{ws} defines the worst solution; and r_1 and r_2 define two random numbers generated within the range of [0, 1]. The step formula (Δx) is given by:

$$\Delta x = 2.rand.|Sp| \tag{7}$$

$$Sp = rand.((\Delta_{best} - rand.\Delta_{avg}) + \alpha)$$

$$\alpha = rand.(\Delta_i - rand.(ub - lb)).exp\left(-4.\frac{it}{T_{max}}\right)$$

where Sp defines the step size; lb and ub defines the lower and upper bounds for the candidate problem; Δ_{avg} stands for the average of solutions during the candidate iteration. Furthermore, Δ_{ws} and Δ_{best} are defined as follows.

$$\begin{aligned} &if\ f(\Delta_i) < f(\Delta_{bs,i}) \\ &\quad \Delta_{best} = \Delta_i \\ &\quad \Delta_{ws} = \Delta_{bs,i} \\ &\quad else \\ &\Delta_{best} = \Delta_{bs,i} \\ &\quad \Delta_{ws} = \Delta_i \\ &\quad end \end{aligned} \tag{8}$$

where $\Delta_{bs,i}$ defines the best solution among three randomly generated members (Δ_{a1}, Δ_{a2}, *and* Δ_{a3}).

2.2. The SEO

To enhance the quality of solutions and avoid using local optima tramping, RUN makes use of an efficient operator, SEO. The RUN algorithm incorporates the SEO operator using the scenarios in Eqs. (9)–(12) to create the solution Δ_{SEO}.

$$\Delta_{SEO} = \begin{cases} \Delta_{new2} + \lambda.\rho.\left|(\Delta_{new2} - \Delta_{avg}) + randn\right| & w < 1 \\ (\Delta_{new2} - \Delta_{avg}) + \lambda.\rho.\left|(2.rand.\Delta_{new2} - \Delta_{avg}) + randn\right| & otherwise \end{cases} \tag{9}$$

$$\rho = rand(0, 2).exp\left(-c\left(\frac{it}{T_{max}}\right)\right) \tag{10}$$

$$\Delta_{avg} = \frac{\Delta_{a1} + \Delta_{a2} + \Delta_{a3}}{3} \tag{11}$$

$$\Delta_{new2} = \gamma \times \Delta_{avg} + (1 - \gamma) \times \Delta_{best} \tag{12}$$

where γ denotes a random number generated within the range of [0, 1], λ stands for an integer number that takes 1, 0, or −1, and c signifies a random number that is set to $5 \times rand$.

Due to the possibility that solution (Δ_{SEO}) may not provide a better fitness function than of the current solution Δ_{new1} (i.e., $f(\Delta_{SEO}) > (\Delta_{new1})$), another hopes of coming up with a promising answer, solution Δ_{new3} is generated, which is considered as follows:

$$\Delta_{new3} = (\Delta_{SEO} - rand_1.\Delta_{SEO}) + SF.(rand_2.\Delta_{IRK} + (2.rand_3.\Delta_{best} - \Delta_{SEO})) \quad (13)$$

where $rand_1$, $rand_2$, and $rand_3$ define random values. The pseudo-code of the conventional RUN is illustrated in Fig. 1.

3. Improved RUN algorithm

By estimating the development of RUN, the RUN algorithm can achieve the best members in search area with the advantages of easy structure and high precision. However, the algorithm still has some drawbacks that may make it prone to signation dilemma while failing to strike a good among the explorative and exploitative features when it comes to dealing with multimodal and complicated concerns [65,66]. Firstly, in RUN algorithm, the search agents are updated in sequential manner using some solutions selected randomly. And then, the weaker ones are eliminated while the better solutions are survival. However, this updating process ignores the self-experience information of the population which may cause the updated members to inherit a high-quality structure. Therefore, a worthwhile challenge is how to ensure that the new population can reach the promising region. Secondly, most optimization approaches suffer from stagnation phenomena, which suck in the local optimal rather than seeking for a better outcome [67]. In a word, Opportunities are offered to enhance the efficiency of the classical RUN. Thus, an improved RUN approach, named IRUN, based on quadratic interpolation strategy (QIS), Laplacian segment mutation (LSM), Levy flight strategy (LFS), and information-sharing-based local search (ISLS) are proposed in this paper.

3.1. The prospective of QIS

The QIS is integrated to enhance the exploitation feature while refining the solution accuracy of RUN algorithm. The QIS uses the approximate polynomial interpolation technique through using the knowledge of the given function at some candidate positions to formulate a low order interpolating polynomial that closely approximates the given objective function, and then use the polynomial's optimal solution as a close approximation of the optimal solution of the given function [68]. Hence, a learning strategy using the function information can enhance the exploration ability. To be specific, the i^{th} individual and its two surrounding individuals $(i+1)^{\text{th}}$, and $(i+2)^{\text{th}}$ are selected, then by using the information of three individuals, a quadratic function can be expressed which is denoted by

Stage 1. Initialization
Initialize the algorithm parameters
Create an initial population randomly within the search bounds (ub, lb)
Stage 2. RUN operators
for $it = 1: T_{max}$
  Evaluate the fitness function of each solution
  Determine the solutions, Δ_{best}, Δ_{cbest}, and Δ_{ws}
  for $j = 1 : d$
    Apply the SM strategy to generate the new solution Δ_{new1} by **Eqs. (1)- (8)**
  end for
  Amend the generated solution using the search bound
  if $f(\Delta_{new1}) < f(\Delta_i)$
    $\Delta_i = \Delta_{new1}$
    $f(\Delta_i) = f(\Delta_{new1})$
  end
  % Solution enhancement operator (SEO)
  if $rand < 0.5$
    Create the position Δ_{SEO} by **Eq. (9)**
  if $f(\Delta_{\text{SEO}}) < f(\Delta_i)$
    $\Delta_i = \Delta_{\text{SEO}}$
    $f(\Delta_i) = f(\Delta_{\text{SEO}})$
  end
  if $rand < \rho$
    Generate the position Δ_{new3} by **Eq. (13)**
  if $f(\Delta_{new3}) < f(\Delta_i)$
    $\Delta_i = \Delta_{new3}$
    $f(\Delta_i) = f(\Delta_{new3})$
  end
  Update Δ_{best}
 end for
end
Output: Return Δ_{best}

Fig. 1. The working steps of the RUN.

$Q(\Delta) = a_0 + a_1\Delta + a_2\Delta^2, a_0, a_1, a_2 \in R$. Let $Q(\Delta)$ represents the interpolating polynomial of the exact function ($f(\Delta)$) at abscissae Δ_i, Δ_{i+1}, Δ_{i+2}. That is.

$$\begin{cases} Q(\Delta_i) = a_0 + a_1\Delta_i + a_2\Delta_i^2 = f(\Delta_i) \\ Q(\Delta_{i+1}) = a_0 + a_1\Delta_{i+1} + a_2\Delta_{i+1}^2 = f(\Delta_{i+1}) \\ Q(\Delta_{i+2}) = a_0 + a_1\Delta_{i+2} + a_2\Delta_{i+2}^2 = f(\Delta_{i+2}) \end{cases} \tag{14}$$

The minimal value of the approximate quadratic function $Q(\Delta)$ can be attained at

$$\Delta^* = \frac{1}{2} \times \frac{(\Delta_{i+1}^2 - \Delta_{i+2}^2)f(\Delta_i) + (\Delta_{i+2}^2 - \Delta_i^2)f(\Delta_{i+1}) + (\Delta_i^2 - \Delta_{i+1}^2)f(\Delta_{i+2})}{(\Delta_{i+1} - \Delta_{i+2})f(\Delta_i) + (\Delta_{i+2} - \Delta_i)f(\Delta_{i+1}) + (\Delta_i - \Delta_{i+1})f(\Delta_{i+2})} \tag{15}$$

By this strategy, an improved solution can be obtained with better fitness value than the previous one. Furthermore, the updating process can be performed using a greedy manner as follows.

$$\begin{cases} \Delta_i^{it+1} = \Delta_i^{it} & f(\Delta_i^{it}) \le f(\Delta_{best}) \\ \Delta_i^{it+1} = \Delta_{best} & f(\Delta_i^{it}) > f(\Delta_{best}) \end{cases} \tag{16}$$

where *it* represents the current iteration of algorithm. After applying the QIS to each individual, the quality of the population can be enriched.

3.2. The prospective of LSM

In IRUN algorithm, the individuals are behaved using some random trends during the SM and SEO stages. This scheme of updating may lead to infective diversification pattern. Therefore, the LSM is adopted at aiming to improve solution' diversity and hence boost the exploration feature [69]. In particular, the LSM is initiated with two individuals, the one of them is selected randomly (Δ_a) and the other one represents the best solution obtained so for (Δ_{best}). Therefore, According to Laplacian distribution, the most probable search pattern is as follows.

$$L_j = \begin{cases} \beta - \gamma\, log_e(u_j) & v_j \le 0.5 \\ \beta - \gamma\, log_e(u_j) & v_j > 0.5 \end{cases} \tag{17}$$

where u_j, v_j stand for two arbitrary numbers generated in the interval $[0, 1]$ using uniform distribution. Here, $\beta \in R$ *and* γ define the location factor and the scaling coefficient, respectively. Thus, the renewed position of the individua can be formulated as given in Eq. (18).

$$\Delta_1^{LSM} = \Delta_a + L \times |\Delta_a - \Delta_{best}| \text{ and } \Delta_2^{LSM} = \Delta_{best} + L \times |\Delta_a - \Delta_{best}| \tag{18}$$

where Δ_1^{LSM} and Δ_1^{LSM} define the new solutions obtained based on LSM. In this regard, LSM establishes fresh solutions in the vicinity of their original ones for a small value of γ, and establishes fresh solutions far from their original ones for the large value of γ. When β and γ are fixed values, the LSM can distribute the new solutions proportional to the parents' distribution.

3.3. The prospective of LFS

To mitigate the loss of diversity with the growth of population and enhance the randomness of the population during the iterative process, the Levy flight strategy (LFS) is adopted as the random walk method based on Levy distribution [70]. LFS is presented to exploit near the solution with promising search ability. According to the LFS, some new solutions can be generated to eliminate the others with poor search ability with the aim to maintain the population 'diversity as well as enable the population to jump out of the local optima. Therefore, the updating process using LFS can be expressed as follows.

$$\Delta_i^{LFS} = \Delta_i.(1 + levy(\beta)) \tag{19}$$

$$\Delta_i = \begin{cases} \Delta_i^{LFS} & f(\Delta_i^{LFS}) < f(\Delta_i) \\ \Delta_i & otherwise \end{cases} \tag{20}$$

where Δ_i^{LFS} defines the renewed position using the LFS, Δ_i defines the present solution, and $levy(\beta)$ denotes the Lévy flight terms that will be illustrated introduced next. Eq. (20) signifies that the present solution is substituted with renewed one based on levy flight perspective if it is better; otherwise, present one is retained. The levy fly step might increase the strength of the algorithm as it is characterized by small and larger jumps steps which improve the exploration and exploitation abilities. From the perspective of implementation, the Mantegna method is used to determine the step size of the Lévy flight [71] as given in Eq. (21):

$$levy(\beta) = \left(\frac{\sigma . u}{|v|^{(1/\beta)}} \right) \tag{21}$$

where u and v represent two parameters drawn from Gaussian distributions as $u \sim N(0,1)$ and $v \sim N(0,1)$ where β defines a distribution index and σ defines the standard deviation that is expressed in Eq. (22).

$$\sigma = \left\{ \frac{\Gamma(1+\beta) sin\left(\frac{\pi\beta}{2}\right)}{\beta . \Gamma\left(\frac{1+\beta}{2}\right) . 2^{\frac{(\beta-1)}{2}}} \right\}^{1/\beta} \tag{22}$$

where $\Gamma(.)$ stands for Gamma function.

3.4. The prospective of ISLS

In the traditional RUN, the local search is carried out in SEO stage using average solution of all solutions. Despite the fact that this update is a useful search tool in some tasks, the solutions are easily trapped at the local optimum challenging with the worse location the population's average. To remedy this shortcoming and strengthen the efficiency of local search, the ISLS is developed to strengthen the exploitation feature through sharing the information of the best leader (Δ^{P}) and worst solution (Δ^{W}) of the elite group within the population. To be specific, the elite group of chosen with identifying the information of Δ_{best}, Δ^{P} and Δ^{W}. Afterwards, the updating process is presented using three types of movements, which are moving Δ^{W} towards Δ^{P}, or moving Δ^{W} towards Δ_{best}, and moving Δ^{W} towards the average of Δ^{P} and Δ_{best}. The movements are performed sequentially and it is stopped when the improved fitness comes to a specific one. The updating process of this stage is as follows:

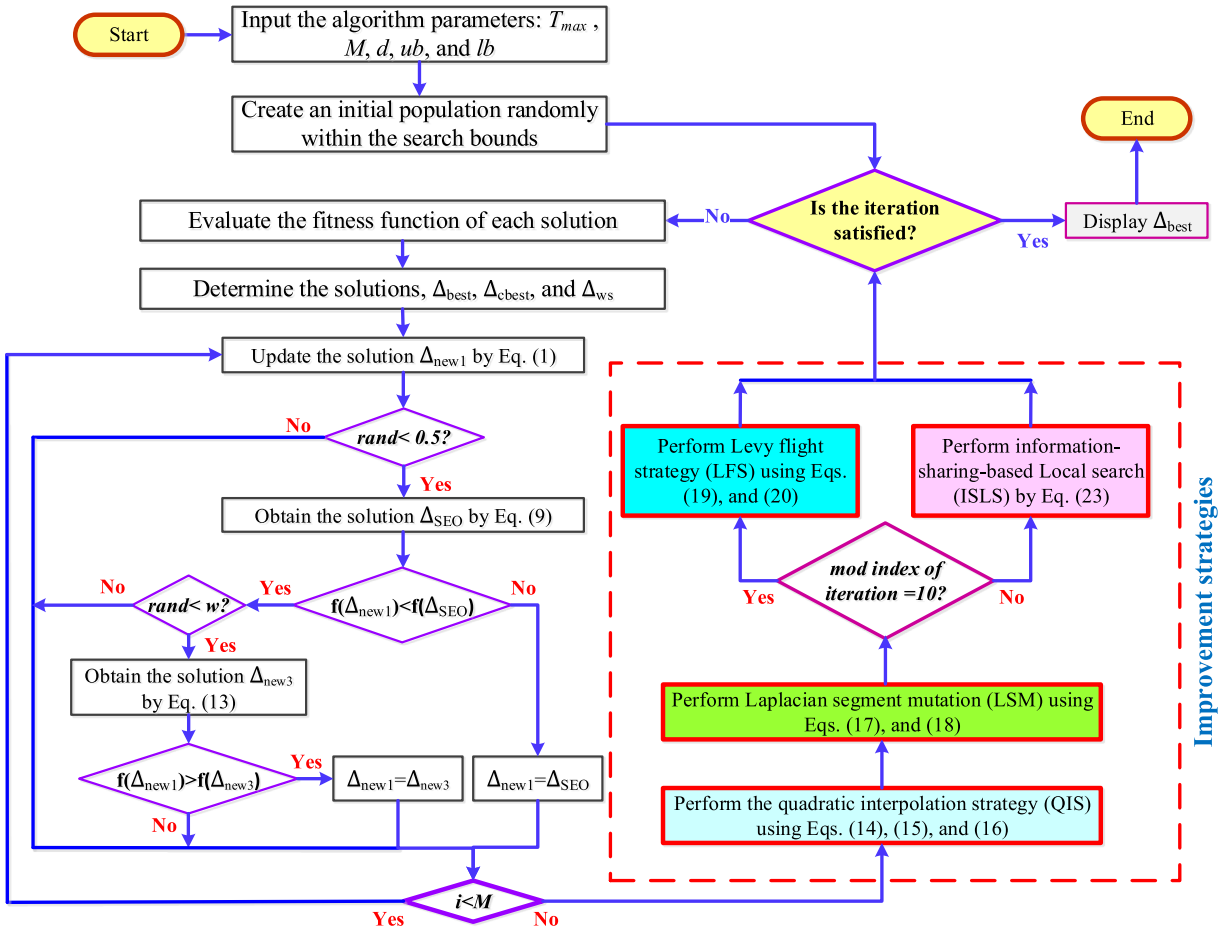


Fig. 2. Flowchart of developed IRUN algorithm.

$$\Delta_I^{it+1} = \begin{cases} \Delta_1^{ISLS} = 2 \times a_1 \times \left(\Delta^P - \Delta^W\right) + \Delta^W & if\ f\left(\Delta_1^{ISLS}\right) \le f\left(\Delta_I^{it}\right) \\ \Delta_2^{ISLS} = 2 \times a_2 \times \left(\Delta_{best} - \Delta^W\right) + \Delta^W & else\ if\ f\left(\Delta_2^{ISLS}\right) \le f\left(\Delta_I^{it}\right) \\ \Delta_3^{ISLS} = 2 \times a_3 \times \left(\left(\Delta^P + \Delta_{best}\right)/2 - \Delta^W\right) + \Delta^W & otherwise \end{cases} \tag{23}$$

where Δ_I^{it} and Δ_I^{it+1} defines the current and updated solutions of the I^{th} individual within the elite group. The flowchart of the proposed IRUN framework is illustrated in Fig. 2.

4. Experimental results on CEC 2020 benchmark functions

In this study we adopt CEC 2020 benchmark functions as a challenging platform for performance evaluation of the proposed IRUN algorithm against well performing and recent optimization algorithms. Table 1 lists the details of the CEC 2020 benchmark suite (F1 to F10). The performance of the IRUN on CEC 2020 benchmark test suite are compared with dwarf mongoose optimization (DMO) algorithm [36], salp swarm algorithm (SSA) [37], grey wolf optimizer (GWO) [38], prairie dog optimization (PDO) algorithm [39], biogeography-based optimization (BBO) [40], particle swarm optimization (PSO) [41], gazelle optimization algorithm (GOA) [42], differential evolution (DE) [43] and sine cosine algorithm (SCA) [44]. For fair comparison purpose, the results listed in Table 2 are obtained with 30 independent runs using a population size of 50 and maximum number of iterations of 1000. Those results demonstrate that the proposed IRUN can statistically reach the best average values (highlighted in bold) for all CEC 2020 benchmark functions, indicating its more excellent capability.

5. Problem definition for photovoltaic cell parameter estimation

Photovoltaic (PV) cells are semiconductor devices that convert sunlight directly into electrical energy. Accurate estimation of PV cell parameters is crucial for the design, analysis, and optimization of photovoltaic systems. These parameters, such as the series resistance, shunt resistance, diode ideality factor, and diode saturation current, play a significant role in determining the overall performance and efficiency of PV cells. To estimate these parameters, researchers and engineers commonly use mathematical models that describe the electrical behavior of PV cells. Two widely used models are the single-diode model and the double-diode model. In this section, we discuss these models and their relevance in the problem of PV cell parameter estimation.

5.1. Single-diode model

The single-diode model (SDM) is a simplified mathematical representation of the electrical characteristics of a PV cell. It assumes that the PV cell can be modeled as a single diode connected in parallel with a current source. The SDM provides a relatively simple and computationally efficient representation of PV cell behavior while capturing the key aspects of its electrical response. In the SDM, the current-voltage (I-V) relationship of a PV cell is described by the following equation:

$$I = I_{ph} \times N_p - I_{sd} \times N_p \times \left[exp\left(\frac{\left(V/N_s + I \times R_s/N_p\right)}{\left(n \times V_t\right)}\right) - 1\right] - \frac{\left(V \times N_p/N_s + I \times R_s\right)}{R_{sh}} \tag{24}$$

where I is the output current of the PV cell, V is the voltage across the PV cell terminals, I_{ph} is the photocurrent generated by the cell under illumination, I_{sd} is the diode saturation current, R_s is the series resistance of the cell, R_{sh} is the shunt resistance of the cell, n is the diode ideality factor, V_t is the thermal voltage, approximately equal to kT/q, where k is Boltzmann's constant, T is the temperature in Kelvin, and q is the elementary charge. In here, N_s represents the number of series diodes and N_s denotes the number of diodes in parallel. In case of a single-diode model, those variables would be $N_s = N_p = 1$. Estimating the parameters of the SDM from measured I-V data involves solving an optimization problem, typically using iterative techniques, to find the values that best fit the observed data. Fig. 3 demonstrates the SDM model of solar PV cell.

Table 1
Details of CEC 2020 test functions [36,39,42].

Function	Type	Definition	Search range	Global
F1	Unimodal	Shifted and Rotated Bent Cigar Function	$[-100, 100]$	100
F2	Basic	Shifted and Rotated Schwefel's Function	$[-100, 100]$	1100
F3		Shifted and Rotated Lunacek bi-Rastrigin Function	$[-100, 100]$	700
F4		Expanded Rosenbrock's plus Griewank's Function	$[-100, 100]$	1900
F5	Hybrid	Hybrid Function 1 ($N = 3$)	$[-100, 100]$	1700
F6		Hybrid Function 2 ($N = 4$)	$[-100, 100]$	1600
F7		Hybrid Function 3 ($N = 5$)	$[-100, 100]$	2100
F8	Composition	Composition Function 1 ($N = 3$)	$[-100, 100]$	2200
F9		Composition Function 2 ($N = 4$)	$[-100, 100]$	2400
F10		Composition Function 3 ($N = 5$)	$[-100, 100]$	2500

Table 2
Statistical results of CEC-2020 test functions

Function	Metric	IRUN	RUN	DMO	SSA	GWO	PDO	BBO	PSO	GOA	DE	SCA
F1	Average	**100**	1190	100.43	2147.5	1.62E+07	100.46	876.9	1692.5	100.43	1759.2	6.96E+08
	Standard Deviation	0	1595.8	0.5024	2274.4	5.88E+07	0.35113	1302.9	1682.6	0.35345	1467.8	3.24E+08
	Best	100	100	100.06	759.13	5729.7	100.06	100.96	100.47	100.04	199.57	100.04
	Worst	100	3776.6	101.8	8959.3	3.20E+08	101.58	5494.9	5621.7	101.51	6437.4	1.91E+09
F2	Average	**1100.2**	1193.9	1126.3	1859.9	1547.3	1241.4	1590.8	1453.2	1246.4	1540.9	2308.3
	Standard Deviation	0.164	61.191	96.47	322.15	204.43	63.833	281.95	171.22	107.35	130.05	224.26
	Best	1100	1107.1	1101.4	1870.4	1121.1	1130.8	1115.2	1118.5	1106.6	1246.5	1106.6
	Worst	1100.6	1367.9	1347	2464	1976.7	1375.1	2263.4	1823.1	1495.8	1804.1	2760.4
F3	Average	**708.22**	713.85	733.22	728.91	728.87	719.69	720.67	720.38	719.59	721.45	776.62
	Standard Deviation	1.5819	3.27	5.1087	12.359	11.928	2.963	4.1885	3.7772	3.0154	2.3513	9.9176
	Best	706	706.94	715.3	725.3	710.94	714.03	714.7	711.97	711.23	716.7	711.23
	Worst	711.6	720.27	742.87	754.19	755.16	724.97	730.06	729.72	724.6	725.64	802.59
F4	Average	**1900**	**1900**	1901.2	1901.7	1902.3	1901.2	1901.5	1901	1901.2	1901.6	1919
	Standard Deviation	0	0	0.54311	0.84053	0.7511	0.3165	0.93587	0.28017	0.31242	0.25486	8.2064
	Best	1900	1900	1900.3	1900.3	1900.7	1900.6	1900.5	1900.5	1900.5	1901.1	1900.5
	Worst	1900	1900	1902.5	1903.9	1903.5	1901.8	1905.1	1901.5	1901.8	1902.2	1941.3
F5	Average	**1706.8**	1712.6	1749	5824.5	19155	1751.3	39375	6326.5	1756.1	28146	31187
	Standard Deviation	5.9331	10.509	18.67	3888.4	69228	16.644	57716	4401.8	16.75	17680	21634
	Best	1701	1702	1715.3	2755.3	2849.3	1720.1	2682.9	1957.2	1734.7	4359.2	1734.7
	Worst	1719.9	1730.8	1819.2	17993	3.85E+05	1797.9	2.18E+05	18436	1799.6	80032	77282
F6	Average	**1600**	1601.4	**1600**	1600.6	1602.4	1600.5	1603.2	1617.2	**1600**	1600.2	1601
	Standard Deviation	0	0.83913	0.000726	0.40604	5.1403	0.001129	5.8731	20.581	0.000893	0.10355	0.21847
	Best	1600	1600.5	1600	1600.1	1600	1600.5	1600.5	1600.5	1600	1600	1600
	Worst	1600	1602.9	1600	1601.2	1617.1	1600.5	1618	1659.5	1600	1600.4	1601.7
F7	Average	**2105.2**	2343.2	2109.3	6181.6	7809.7	2108	9666.2	2741.6	2110	3340.3	7865
	Standard Deviation	8.5224	211.95	9.74	5670.6	4502.9	4.5969	7064.8	746.11	5.5831	1260.2	3543
	Best	2100	2131.4	2103.8	2263.8	2520.4	2101.5	2121.4	2101.8	2102.9	2271.8	2102.9
	Worst	2122.3	2743.6	2178.5	26256	15961	2122.5	24664	5640.2	2122.5	8615.2	15558
F8	Average	**2235.5**	2241.1	2269.4	2300.4	2308.5	2278.3	2299.4	2302.4	2286.7	2298.8	2374.9
	Standard Deviation	47.984	44.057	14.228	14.146	29.134	43.878	14.607	1.0982	35.252	7.5443	39.318
	Best	2200	2200	2200.1	2234.3	2212	2200	2222.3	2301.1	2200.2	2261.9	2200.2
	Worst	2304.4	2303.9	2303.3	2307.6	2426.5	2304.4	2304.2	2305.1	2303.5	2302.1	2502
F9	Average	**2500**	2747.9	2525	2740.3	2740.7	2559.5	2722.1	2717.7	2523.3	2737	2774.8
	Standard Deviation	0	8.9794	27.203	46.254	38.126	83.741	75.875	74.071	67.32	23.448	40.458
	Best	2500	2735.6	2500	2500	2546.9	2500	2500	2500	2418.4	2646.2	2418.4
	Worst	2500	2769.3	2590.2	2778.4	2763	2739.7	2773.4	2753.9	2734.1	2755.4	2798.3
F10	Average	**2764.9**	2848.8	2803.2	2923.7	2938	2887.9	2930.5	2924.7	2871.8	2918.5	2962.1
	Standard Deviation	118.62	7.6462	9.2352	24.085	14.205	53.863	23.126	23.104	80.727	14.58	12.341
	Best	2600	2847.4	2598.1	2898.1	2903.5	2602.7	2897.7	2898.1	2601.3	2899.2	2601.3
	Worst	2847.4	2889.3	2844.4	2949	2949.7	2897.8	2948.9	2946	2897.8	2946.6	2988.6

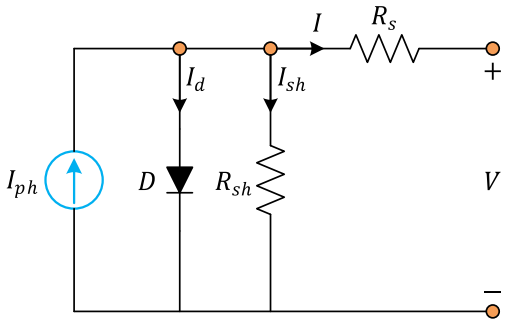


Fig. 3. SDM of solar PV cell.

5.2. Double-diode model

The double-diode model (DDM) is an advanced PV cell model that incorporates additional diodes to account for more complex electrical behavior. It introduces an additional diode to represent the recombination losses in the PV cell and provides a more accurate description of real-world PV cell characteristics. In the DDM, the I-V relationship of a PV cell is described by the following equation:

$$I = I_{ph} \times N_p - I_{sd1} \times N_p \times \left[exp\left(\frac{\left(V/N_s + I \times R_s/N_p\right)}{(n_1 \times V_t)} \right) - 1 \right] - I_{sd2} \times N_p \times \left[exp\left(\frac{\left(V/N_s + I \times R_s/N_p\right)}{(n_2 \times V_t)} \right) - 1 \right] - \frac{\left(V \times N_p/N_s + I \times R_s\right)}{R_{sh}} \tag{25}$$

where I_{sd1} is the diode saturation current of the main diode, I_{sd2} is the diode saturation current of the additional diode, n_1 is the ideality factor of the main diode and n_2 is the ideality factor of the additional diode. In here, N_s represents the number of series diodes and N_s denotes the number of diodes in parallel. In case of a double-diode model, those variables would be $N_s = 1$ and $N_p = 2$. Estimating the parameters of the DDM requires solving an optimization problem that minimizes the difference between the measured I-V data and the modeled I-V curve based on the DDM equation. This optimization process involves adjusting the values of the parameters until a good fit between the model and the measured data is achieved. Fig. 4 demonstrates the DDM model of solar PV cell.

Compared to the SDM, the DDM provides a more accurate representation of the electrical characteristics of PV cells, particularly in situations where recombination losses are significant. However, due to the additional complexity of the model, parameter estimation for the DDM can be more computationally intensive and requires more measurement data points to achieve reliable results.

5.3. Objective function

In the process of PV cell parameter estimation, an objective function is essential to quantify the accuracy of the estimated parameters by comparing the modeled I-V curve with the measured data. Two commonly used objective functions for evaluating the goodness-of-fit are root mean squared error (*RMSE*) and mean absolute error (*MAE*). *RMSE* is a popular metric that measures the average magnitude of the differences between the modeled and measured values. It calculates the square root of the mean of the squared differences between each data point of the measured I-V curve (I_m) and the corresponding point of the modeled I-V curve ($I_{modeled}$), given a set of estimated parameters:

$$RMSE = \sqrt{\frac{1}{N} \sum_{i=1}^{N} \left(I_{measured} - I_{modeled}\right)^2} \tag{26}$$

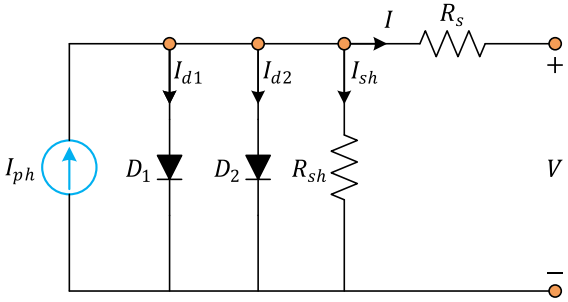


Fig. 4. DDM of solar PV cell.

where N is the total number of data points. *RMSE* provides a comprehensive measure of the overall discrepancy between the model and the measured data. To estimate the current, the nonlinear equations derived from the equivalent circuits (Eq. (24) and (25) can be solved. In the conventional objective function, given a voltage measurement and a current measurement, the current is estimated using the following expression:

$$I_{modeled} = I_{ph} - I_{sd}\left[e^{\frac{(V+I_{measured}R_s)}{(nV_t)}} - 1\right] - \frac{(V + I_{measured}R_s)}{R_{sh}} \tag{27}$$

Substituting Eq. (27) into Eq. (24), will lead to Eq. (28) for the SDM:

$$F_{Obj} = \sqrt{\frac{1}{N}\sum_{i=1}^{N}\left(I_{measured} - \left\{I_{ph} - I_{sd}\left[e^{\frac{(V+I_{measured}R_s)}{(nV_t)}} - 1\right] - \frac{(V + I_{measured}R_s)}{R_{sh}}\right\}\right)^2} \tag{28}$$

For the DDM, this will be as in Eq. (29):

$$F_{Obj} = \sqrt{\frac{1}{N}\sum_{i=1}^{N}\left(I_{measured} - \left\{I_{ph} - I_{sd1}\left[e^{\frac{(V+I_{measured}R_s)}{(n_1V_t)}} - 1\right] - I_{sd2}\left[e^{\frac{(V+I_{measured}R_s)}{(n_2V_t)}} - 1\right] - \frac{(V + I_{measured}R_s)}{R_{sh}}\right\}\right)^2} \tag{29}$$

The RMSE penalizes larger errors more heavily due to the squaring operation, which can be useful when outliers or extreme values have a significant impact on the analysis. The lower the *RMSE* value, the better the agreement between the model and the measurements. *MAE* is another widely used metric for assessing the accuracy of parameter estimation. Unlike *RMSE*, *MAE* (Eq. (30)) calculates the average magnitude of the absolute differences between the measured and modeled values:

$$MAE = \frac{1}{N}\sum_{i=1}^{N}|I_{measured} - I_{modeled}| \tag{30}$$

where N is the total number of data points. *MAE* provides a measure of the average absolute discrepancy between the model and the measured data. It is less sensitive to outliers compared to *RMSE* since it does not involve squaring the differences. *MAE* is useful when a balanced evaluation of errors is desired, and extreme values should not disproportionately affect the assessment. Similar to *RMSE*, a lower *MAE* value indicates a better fit between the model and the measurements.

6. Experimental results on PV models

In order to evaluate the effectiveness of the proposed IRUN technique, we applied it to estimate the parameters of various equivalent circuit models for both solar cells and PV modules. Specifically, we considered the SDM model with 5 parameters and the DDM model with 7 parameters. Two case studies were conducted to assess the performance of the technique. For the first case study, we utilized a standard experimental dataset obtained from a commercial R.T.C. France silicon solar cell [72] operating at a temperature of 33°C and a solar radiance of 1000 W/m^2. For the R.T.C. France silicon solar cell, the N_s value is taken as 1.

In the second case study, we employed an experimental dataset derived from an industrial solar module known as CS6P-220P, which operates at 30 °C and a solar radiance of 1000 W/m^2. The CS6P-220P PV module consists of 6×10 polycrystalline solar cells connected in series, with a rated maximum power of 220 W. This PV system, depicted in Fig. 5, was installed at the Engineering Faculty of Düzce University in Turkey. Although the system contains multiple solar modules for power enhancement, our focus was on a single module, which was isolated from the system. For the CS6P220P solar module, the N_s value is taken as 60.

In addition to the previously discussed models, this study extends its evaluation of the proposed method's efficacy by incorporating



Fig. 5. The used solar PV module at the Engineering Faculty of Düzce University in Turkey.

two additional and distinct photovoltaic systems. Specifically, the investigation includes an in-depth analysis of a three-diode model representing the characteristics of the R.T.C. France solar cell. Furthermore, the study delves into the intricacies of a photovoltaic module, focusing on the STM6-40/36 PV module. For the STM6-40/36 PV module, the N_s value is taken as 36. By incorporating these diverse models into the assessment framework, this study aims to provide a comprehensive understanding of the proposed method's versatility and robustness across varied photovoltaic technologies.

To ensure a fair comparison, we set the population size to 30 and the maximum number of iterations to 400. The algorithms were executed 30 times for each case study. Due to its high accuracy and less computational burden, this study adopts the iterative Newton–Raphson method [73] for parameters extraction. Therefore, the proposed IRUN algorithm runs in coordination with the Newton - Raphson method and uses the dataset by evaluating RMSE objective function value. The explained parameter estimation procedure employed in this study is illustrated in Fig. 6.

6.1. Experimental results for first case study

6.1.1. Single-diode model

Initial evaluation of the proposed IRUN algorithm is initially performed using the SDM model of the commercially available and widely adopted commercial R.T.C. France silicon solar cell. The specifications of the SDM parameters employed for this study are presented in Table 3. The latter table also provides the optimized parameter values using the standard form of RUN algorithm and the proposed IRUN algorithm. The statistical metrics, such as average, standard deviation, best and worst, obtained for the RMSE values are displayed in this table, as well. As shown with the bold values the proposed IRUN algorithm helps reaching lower statistical values indicating greater capability of the proposed methodology.

The scatter plot demonstrating the distribution of the RMSE objective function value obtained for each run number of RUN and IRUN algorithms using SDM model of R.T.C France solar cell is displayed in Fig. 7. As can be observed from the illustration in Fig. 7, the proposed IRUN algorithm consistently reaches the lowest RMSE values compared to the standard version of RUN algorithm. Besides, IRUN algorithm has a lower standard deviation indicating its robust nature in terms of reaching good quality solutions.

Convergence rates of the standard RUN and proposed IRUN algorithms for the SDM model of the commercially available R.T.C France solar cell are displayed in Fig. 8. As can be observed from the convergence curves, both algorithms tend to reach lower RMSE values, however, the proposed IRUN algorithm is capable of reaching the lowest RMSE value and the best solution in earlier iterations. The optimized parameters obtained through the RUN and IRUN algorithms using SDM method were used to estimate the I-V and P-V characteristics of the R.T.C. France silicon solar cell. Fig. 9 illustrates the close match between the estimated data and the experimental data across the entire voltage range. Here, Fig. 9 (a) displays the I-V characteristics and Fig. 9 (b) shows the P-V characteristics.

The sampled 26 voltage and current values obtained from the R.T.C France solar cell are provided in Table 4. This table also displays the estimated current and absolute current error values optimized by RUN and IRUN algorithms using single-diode model. As can be seen, the proposed IRUN algorithm reaches lowest RMSE value, outperforming the performance of the standard RUN algorithm. In terms of MAE value, there is no significant difference between the standard RUN and the proposed IRUN algorithms.

To highlight the efficacy of the IRUN algorithm for the parameter estimation of the R.T.C France silicon solar cell using single-diode model, we adopted state-of-the-art approaches reported in recent literature. In this context, the algorithms listed in Table 5 (squirrel search algorithm (SSA) [15], elite learning adaptive differential evolution (ELADE) [45], hybrid multi-group stochastic cooperative particle swarm optimization (HMSCPSO) [46], queuing search optimization and differential evolution (IQSODE) [47], hybrid chaotic northern goshawk and pattern search (CNGPS) [48], hybrid chimp algorithm (ChOA) [49], flexible improved particle swarm

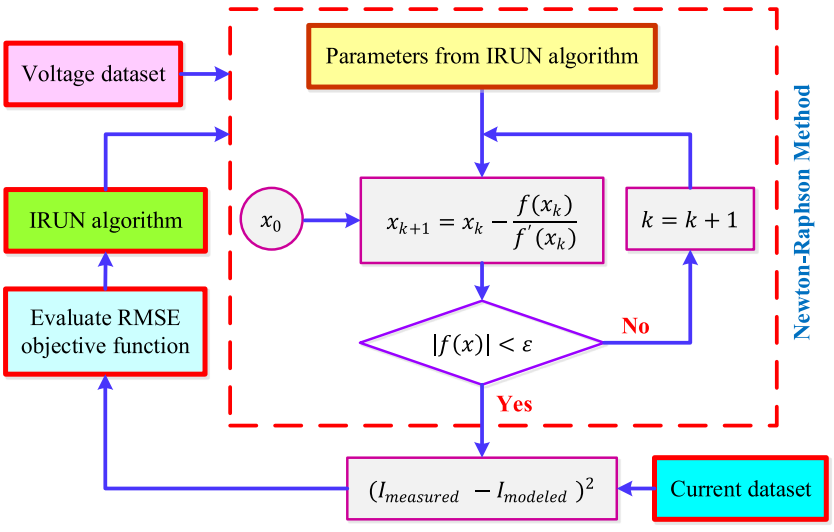


Fig. 6. Illustration of parameter estimation by integrating Newton-Raphson method with IRUN algorithm.

Table 3
Bounds [15,28,32,45–64] and optimized values of SDM parameters for R.T.C France solar cell

Parameter	Lower bound	Upper Bound	Optimized by RUN	Optimized by IRUN
I_{ph} (A)	0	1	0.7608	0.7608
I_{sd} (A)	0	1E−06	3.1973E−07	3.1069E−07
R_s (Ω)	0	0.5	0.0364	0.0365
R_{sh} (Ω)	0	100	53.7850	52.8899
n	1	2	1.4801	1.4773
RMSE	Average		7.8293E−04	**7.7299E−04**
	Standard Deviation		6.0315E−06	**3.0513E−09**
	Best		7.7456E−04	**7.7299E−04**
	Worst		7.9180E−04	**7.7300E−04**

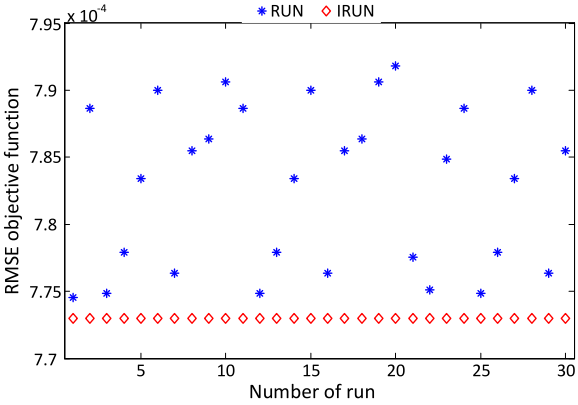


Fig. 7. Scatter plot.

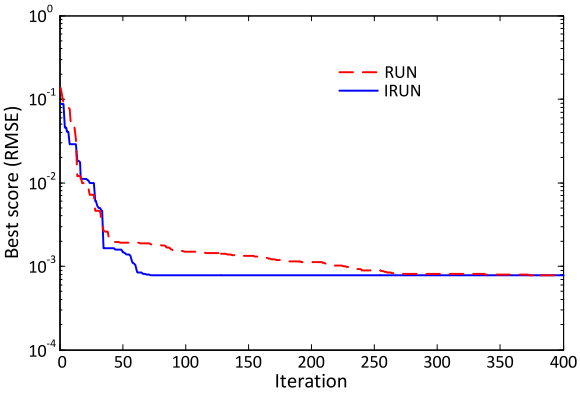


Fig. 8. Convergence rates of RUN and IRUN algorithms for SDM model of R.T.C France solar cell.

optimization and sequential quadratic programming (FIPSO-SQP) [50], weighted mean of vectors algorithm (INFO) [51], differential evolution (DE) [52], sine cosine differential gradient based optimizer (SDGBO) [53], quantum Nelder-Mead hunger games search algorithm (IHGS) [54], improved tunicate swarm algorithm (ITSA) [55], enhanced Harris hawk optimization (EHHO) [56], gradient based optimization with ranking mechanisms (EGBO) [57], stochastic fractal search algorithm (SFS) [58], coyote optimization algorithm (COA) [59], improved Lozi map based chaotic optimization algorithm (ILCOA) [60], improved moth-flame optimization (IMFO) [61], hybrid firefly and pattern search algorithm (HFAPS) [62], improved jaya optimization algorithm (IJAYA) [63], artificial bee colony optimization (ABC) [64], conscious neighborhood strategy-based Laplacian barnacles mating algorithm (NLBMA) [28] and war strategy optimization (WSO) [32]) were used as 23 different and efficient competitors for comparison. As can be observed the proposed IRUN algorithm reaches the lowest RMSE value (highlighted in bold) when using the SDM demonstrating its greater efficacy compared to the recently reported effective approaches.

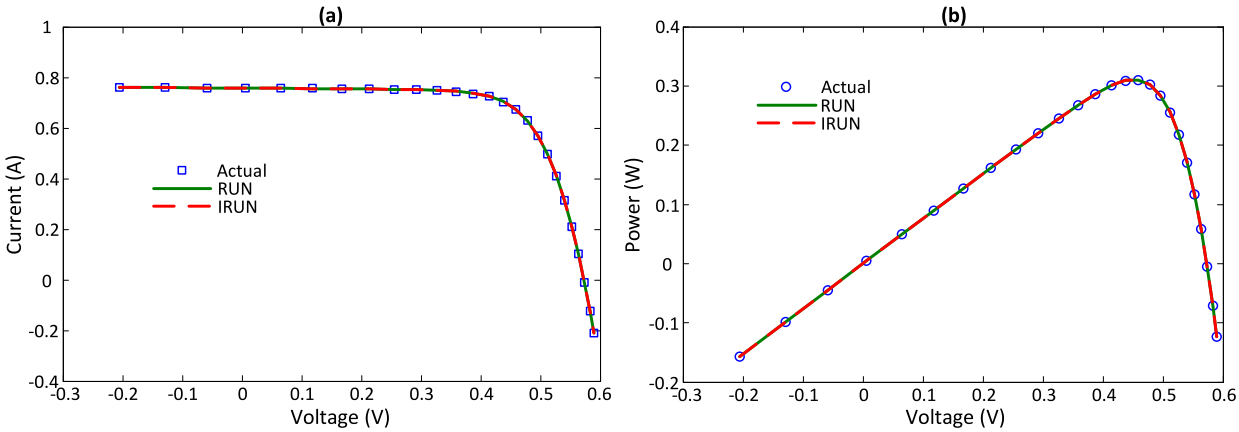


Fig. 9. Characteristics of R.T.C France solar cells using RUN and IRUN algorithms for SDM.

Table 4
Experimental and estimated current data for R.T.C France silicon solar cell (SDM)

Data no	Voltage (V)	Actual current (A)	Optimized by RUN		Optimized by IRUN	
			Estimated current (A)	Absolute current error (A)	Estimated current (A)	Absolute current error (A)
1	−0.2057	0.7640	0.7641	0.0001	0.7641	0.0001
2	−0.1291	0.7620	0.7627	0.0007	0.7627	0.0007
3	−0.0588	0.7605	0.7614	0.0009	0.7614	0.0009
4	0.0057	0.7605	0.7602	0.0003	0.7602	0.0003
5	0.0646	0.7600	0.7591	0.0009	0.7590	0.0010
6	0.1185	0.7590	0.7580	0.0010	0.7580	0.0010
7	0.1678	0.7570	0.7571	0.0001	0.7570	0.0000
8	0.2132	0.7570	0.7561	0.0009	0.7561	0.0009
9	0.2545	0.7555	0.7551	0.0004	0.7550	0.0005
10	0.2924	0.7540	0.7537	0.0003	0.7536	0.0004
11	0.3269	0.7505	0.7514	0.0009	0.7513	0.0008
12	0.3585	0.7465	0.7474	0.0009	0.7473	0.0008
13	0.3873	0.7385	0.7401	0.0016	0.7401	0.0016
14	0.4137	0.7280	0.7274	0.0006	0.7274	0.0006
15	0.4373	0.7065	0.7070	0.0005	0.7070	0.0005
16	0.4590	0.6755	0.6754	0.0001	0.6754	0.0001
17	0.4784	0.6320	0.6309	0.0011	0.6310	0.0010
18	0.4960	0.5730	0.5721	0.0009	0.5722	0.0008
19	0.5119	0.4990	0.4995	0.0005	0.4995	0.0005
20	0.5265	0.4130	0.4135	0.0005	0.4135	0.0005
21	0.5398	0.3165	0.3172	0.0007	0.3172	0.0007
22	0.5521	0.2120	0.2121	0.0001	0.2120	0.0000
23	0.5633	0.1035	0.1027	0.0008	0.1026	0.0009
24	0.5736	−0.0100	−0.0092	0.0008	−0.0093	0.0007
25	0.5833	−0.1230	−0.1244	0.0014	−0.1244	0.0014
26	0.5900	−0.2100	−0.2091	0.0009	−0.2091	0.0009
MAE			**6.7806E−04**		6.7815E−04	
RMSE (objective function)			7.7456E−04		**7.7299E−04**	

6.1.2. Double-diode model

The evaluation of the proposed IRUN algorithm is also performed using the DDM model of the commercially available and widely adopted commercial R.T.C. France silicon solar cell. The specifications of the DDM parameters employed for this study are presented in Table 6. The latter table also provides the optimized parameter values using the standard form of RUN algorithm and the proposed IRUN algorithm. The statistical metrics, such as average, standard deviation, best and worst, obtained for the RMSE values are displayed in this table, as well. As shown with the bold values the proposed IRUN algorithm helps reaching lower statistical values indicating greater capability of the proposed methodology.

The scatter plot demonstrating the distribution of the RMSE objective function value obtained for each run number of RUN and IRUN algorithms using DDM model of R.T.C France solar cell is displayed in Fig. 10. As can be observed from the illustration in Fig. 10, the proposed IRUN algorithm consistently reaches the lowest RMSE values compared to the standard version of RUN algorithm. indicating its superiority in terms of reaching good quality solutions.

Convergence rates of the standard RUN and proposed IRUN algorithms for the DDM model of the commercially available R.T.C

Table 5
Comparative performance assessment in terms of estimating the SDM parameters of R.T.C France silicon solar cell

Method	I_{ph} (A)	I_{sd} (A)	R_s (Ω)	R_{sh} (Ω)	n	*RMSE*
IRUN (proposed)	0.7608	3.1069E−07	0.0365	52.8899	1.4773	**7.7299E−04**
RUN (proposed)	0.7608	3.1973E−07	0.0364	53.7850	1.4801	7.7456E−04
SSA [15]	0.7608	3.0512E−07	0.0366	52.6053	1.4754	7.7551E−04
ELADE [45]	0.7608	3.2302E−07	0.0364	53.7185	1.4812	9.8602E−04
HMSCPSO [46]	0.7608	3.2302E−07	0.0364	53.7185	1.4812	9.8602E−04
IQSODE [47]	0.7608	3.2302E−07	0.0364	53.7185	1.4812	9.8602E−04
CNGPS [48]	0.7608	3.2302E−07	0.0364	53.7185	1.4812	9.8602E−04
ChOA [49]	0.7608	3.2290E−07	0.0364	53.7187	1.4811	9.7601E−04
FIPSO-SQP [50]	0.7608	3.2267E−07	0.0364	53.6880	1.4810	9.8602E−04
INFO [51]	0.7608	3.2300E−07	0.0364	53.7185	1.4812	9.8602E−04
DE [52]	0.7607	3.2090E−07	0.0363	54.1134	1.4709	7.7692E−04
SDGBO [53]	0.7608	3.2302E-07	0.0364	53.7185	1.4812	9.8602E−04
IHGS [54]	0.7608	3.2302E−07	0.0364	53.7178	1.4812	9.8602E−04
ITSA [55]	0.7683	3.2620E−07	0.0367	54.2557	1.4958	9.8600E−04
EHHO [56]	0.7608	3.2300E−07	0.0364	53.7191	1.4769	9.8602E−04
EGBO [57]	0.7608	3.2300E−07	0.0364	53.7185	1.4811	9.8602E−04
SFS [58]	0.7609	3.1670E−07	0.0365	53.2805	1.4792	7.9310E−04
COA [59]	0.7608	3.0839E−07	0.0366	52.8267	1.4765	7.7547E−04
ILCOA [60]	0.7608	3.2302E−07	0.0364	53.7187	1.4811	9.8602E−04
IMFO [61]	0.7608	3.2296E−07	0.0364	53.7146	1.4812	9.8602E−04
HFAPS [62]	0.7608	3.2262E−07	0.0364	53.6784	1.4811	9.8602E−04
IJAYA [63]	0.7608	3.2280E−07	0.0364	53.7595	1.4811	9.8603E−04
ABC [64]	0.7608	3.2510E−07	0.0364	53.6433	1.4817	9.8620E−04
NLBMA [28]	0.7608	3.1068E−07	0.0365	52.8898	1.5177	7.7301E−04
WSO [32]	0.7608	3.1068E−07	0.0365	52.8898	1.4773	7.7301E−04

Table 6
Bounds [15,28,32,45–64] and optimized values of DDM parameters for R.T.C France solar cell

Parameter	Lower Bound	Upper Bound	Optimized by RUN	Optimized by IRUN
I_{ph} (A)	0	1	0.7607	0.7608
I_{sd1} (A)	0	1E−06	2.2028E−07	1.0000E−06
I_{sd2} (A)	0	1E−06	5.1612E−07	8.9071E−08
R_s (Ω)	0	0.5	0.0367	0.0376
R_{sh} (Ω)	0	100	57.1164	55.9993
n_1	1	2	1.4506	1.8239
n_2	1	2	1.8788	1.3804
RMSE	Average		7.7452E−04	**7.5186E−04**
	Standard Deviation		**4.0155E−06**	6.4647E−06
	Best		7.6882E−04	**7.4213E−04**
	Worst		7.8350E−04	**7.6537E−04**

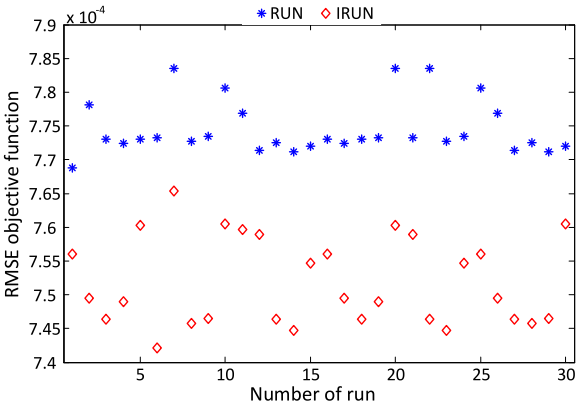


Fig. 10. Scatter plot.

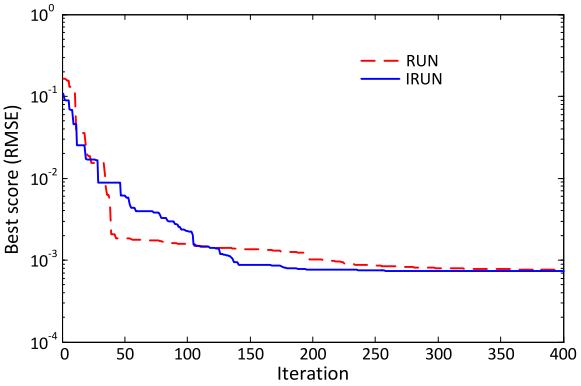


Fig. 11. Convergence rates of RUN and IRUN algorithms for DDM model of the R.T.C France solar cell.

France solar cell are displayed in Fig. 11. As can be observed from the convergence curves, both algorithms tend to reach lower RMSE values, however, the proposed IRUN algorithm is capable of reaching the lowest RMSE value and good solution in earlier iterations. The optimized parameters obtained through the RUN and IRUN algorithms using DDM method were used to estimate the I-V and P-V characteristics of the R.T.C. France silicon solar cell. Fig. 12 illustrates the close match between the estimated data and the experimental data across the entire voltage range. Here, Fig. 12 (a) displays the I-V characteristics and Fig. 12 (b) shows the P-V characteristics.

The experimental 26 voltage and current values obtained from the R.T.C France solar cell using double-diode model are provided in Table 7. This table also displays the estimated current and absolute current error values optimized by RUN and IRUN algorithms using double-diode model. As can be seen, the proposed IRUN algorithm reaches the lowest RMSE and MAE values, outperforming the performance of the standard RUN algorithm for the DDM case.

To highlight the efficacy of the IRUN algorithm for the parameter estimation of the R.T.C France silicon solar cell using double-diode model, we adopted state-of-the-art approaches reported in recent literature. In this context, the algorithms listed in Table 8 were used as 23 different and efficient competitors for comparison. As can be observed the proposed IRUN algorithm reaches the lowest RMSE value (highlighted in bold) when using the DDM demonstrating its greater efficacy compared to the recently reported effective approaches.

6.2. *Experimental results for second case study*

6.2.1. *Single-diode model*

By leveraging the acquired experimental dataset from the CS6P-220P PV module, we have employed the IRUN algorithm to estimate the unknown parameters of both the single-diode model and double-diode model associated with this solar module. Table 9 reveals the bounds [15] and optimized values of SDM parameters for CS6P-220P PV module. This table also demonstrates the improvements achieved through IRUN methodology, as evidenced by the statistical values of the RMSE. It is worth noting that the diode ideality factor (n), series (R_s) and shunt (R_{sh}) resistance values provided in Table 9 represent the cumulative values for all cells. For individual cells, the diode ideality factor and resistance values are determined by dividing them by the number of cells in series (N_s).

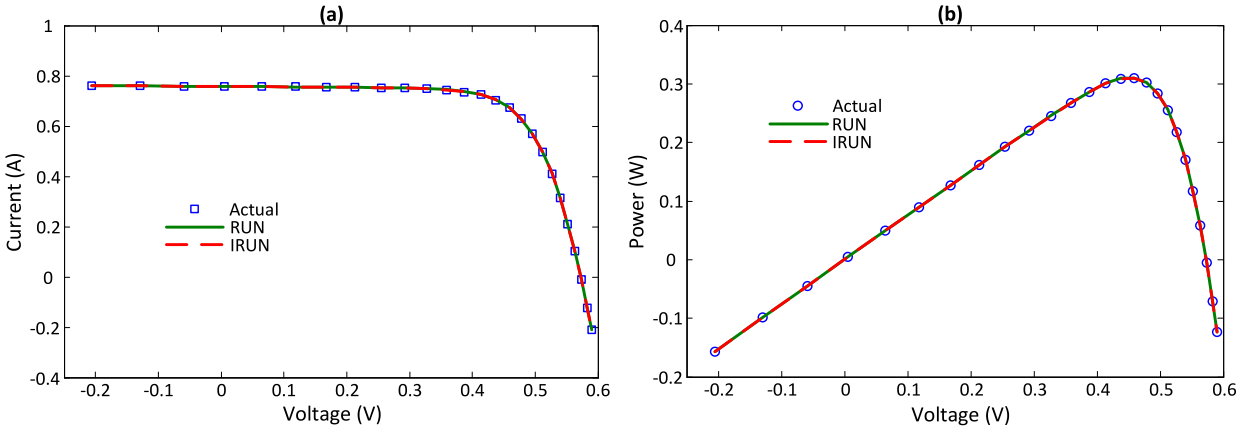


Fig. 12. Characteristics of R.T.C France solar cells using RUN and IRUN algorithms for DDM.

Table 7
Experimental and estimated current data for R.T.C France silicon solar cell (DDM)

Data no	Voltage (V)	Actual current (A)	Optimized by RUN		Optimized by IRUN	
			Estimated current (A)	Absolute current error (A)	Estimated current (A)	Absolute current error (A)
1	−0.2057	0.7640	0.7638	0.0002	0.7640	0.0000
2	−0.1291	0.7620	0.7625	0.0005	0.7626	0.0006
3	−0.0588	0.7605	0.7613	0.0008	0.7613	0.0008
4	0.0057	0.7605	0.7601	0.0004	0.7602	0.0003
5	0.0646	0.7600	0.7591	0.0009	0.7591	0.0009
6	0.1185	0.7590	0.7582	0.0008	0.7582	0.0008
7	0.1678	0.7570	0.7572	0.0002	0.7572	0.0002
8	0.2132	0.7570	0.7563	0.0007	0.7563	0.0007
9	0.2545	0.7555	0.7553	0.0002	0.7552	0.0003
10	0.2924	0.7540	0.7539	0.0001	0.7537	0.0003
11	0.3269	0.7505	0.7516	0.0011	0.7513	0.0008
12	0.3585	0.7465	0.7475	0.0010	0.7472	0.0007
13	0.3873	0.7385	0.7402	0.0017	0.7399	0.0014
14	0.4137	0.7280	0.7274	0.0006	0.7272	0.0008
15	0.4373	0.7065	0.7069	0.0004	0.7068	0.0003
16	0.4590	0.6755	0.6753	0.0002	0.6753	0.0002
17	0.4784	0.6320	0.6309	0.0011	0.6311	0.0009
18	0.4960	0.5730	0.5721	0.0009	0.5724	0.0006
19	0.5119	0.4990	0.4995	0.0005	0.4997	0.0007
20	0.5265	0.4130	0.4135	0.0005	0.4136	0.0006
21	0.5398	0.3165	0.3172	0.0007	0.3172	0.0007
22	0.5521	0.2120	0.2120	0.0000	0.2119	0.0001
23	0.5633	0.1035	0.1026	0.0009	0.1024	0.0011
24	0.5736	−0.0100	−0.0093	0.0007	−0.0095	0.0005
25	0.5833	−0.1230	−0.1245	0.0015	−0.1244	0.0014
26	0.5900	−0.2100	−0.2092	0.0008	−0.2089	0.0011
MAE			6.6187E−04		**6.5422E−04**	
RMSE (objective function)			7.6882E−04		**7.4213E−04**	

Table 8
Comparative performance assessment in terms of estimating the DDM parameters of R.T.C France silicon solar cell

Method	I_{ph} (A)	I_{sd1} (A)	I_{sd2} (A)	R_s (Ω)	R_{sh} (Ω)	n_1	n_2	RMSE
IRUN (proposed)	0.7608	1.0000E−06	8.9071E−08	0.0376	55.9993	1.8239	1.3804	**7.4213E−04**
RUN (proposed)	0.7607	2.2028E−07	5.1612E−07	0.0367	57.1164	1.4506	1.8788	7.6882E−04
SSA [15]	0.7608	1.0000E−06	3.0561E−07	0.0364	55.3636	2.5000	1.4763	7.7192E−04
ELADE [45]	0.7608	2.2598E−07	7.4932E−07	0.0367	55.4855	1.4510	2	9.8248E−04
HMSCPSO [46]	0.7608	7.7600E−07	2.2300E−07	0.0368	55.5555	2	1.4499	9.8249E−04
IQSODE [47]	0.7608	7.4934E−07	2.2597E−07	0.0367	55.4854	2	1.4510	9.8248E−04
CNGPS [48]	0.7608	6.9844E−07	2.3182E−07	0.0367	55.3700	1.9999	1.4535	9.8251E−04
ChOA [49]	0.7608	2.2290E−07	7.2718E−07	0.0364	55.4264	1.4512	2	9.7201E−04
FIPSO-SQP [50]	0.7608	5.9149E−07	2.4051E−07	0.0367	53.8414	2	1.4547	9.8177E−04
INFO [51]	0.7608	5.8760E−07	2.4520E−07	0.0367	55.1368	2	1.4578	9.8268E−04
DE [52]	0.7605	4.2322E−07	1.8726E−07	0.0206	51.9345	1.8758	1.4360	7.6300E−04
SDGBO [53]	0.7608	5.0569E−07	2.5570E−07	0.0366	54.9246	2	1.4614	9.8270E−04
IHGS [54]	0.7608	7.4935E−07	2.2597E−07	0.0367	55.4854	2	1.4510	9.8248E−04
ITSA [55]	0.7608	9.7310E−07	1.6790E−07	0.0369	53.8368	1.9213	1.4281	9.8200E−04
EHHO [56]	0.7608	3.2100E−07	2.3400E−08	0.0364	53.8400	1.4764	2	9.8584E−04
EGBO [57]	0.7608	2.2500E−07	7.4900E−07	0.0367	55.4855	1.4510	2	9.8248E−04
SFS [58]	0.7608	2.1830E−07	3.6810E−07	0.0367	54.5464	1.4500	1.8200	7.7827E−04
COA [59]	0.7607	2.4468E−07	3.8019E−07	0.0369	53.5130	1.4564	1.9899	7.6480E−04
ILCOA [60]	0.7608	2.2601E−07	7.4921E−07	0.0367	55.5320	1.4510	2	9.8257E−04
IMFO [61]	0.7608	2.3350E−07	6.8372E−07	0.0367	55.2997	1.4537	2	9.8252E−04
HFAPS [62]	0.7608	2.2597E−07	7.4936E−07	0.0367	55.4855	1.4510	2	9.8248E−04
IJAYA [63]	0.7601	5.0445E−09	7.5094E−07	0.0376	77.8519	1.2186	1.6247	9.8293E−04
ABC [64]	0.7608	4.0700E−08	2.8740E−07	0.0364	53.7804	1.4495	1.4885	9.8610E−04
NLBMA [28]	0.7605	8.2300E−08	1.8092E−06	0.0380	60.9892	1.4078	2	7.5242E−04
WSO [32]	0.7608	9.6909E−08	9.9998E−07	0.0376	55.9659	1.3863	1.8351	7.5991E−04

The scatter plot demonstrating the distribution of the RMSE objective function value obtained for each run number of RUN and IRUN algorithms using SDM model of CS6P-220P PV module is displayed in Fig. 13. As can be observed from the illustration in Fig. 13, the proposed IRUN algorithm consistently reaches the lowest RMSE values compared to standard version of RUN algorithm. Besides, IRUN algorithm has a lower standard deviation indicating its robust nature in terms of reaching good quality solutions.

Table 9
Bounds [15] and optimized values of SDM parameters for CS6P-220P PV module

Parameter	Lower Bound	Upper Bound	Optimized by RUN	Optimized by IRUN
I_{ph} (A)	6	9	7.9722	7.9372
I_{sd} (A)	1E−35	1E−28	1.0000E−28	1.0000E−28
R_s (Ω)	0.25	2	0.8566	0.8492
R_{sh} (Ω)	30	60	30.0000	30.3157
n	10	25	19.2391	19.2309
RMSE	Average		5.2848E−02	**4.9841E−02**
	Standard Deviation		8.8689E−04	**1.4115E−17**
	Best		5.1977E−02	**4.9841E−02**
	Worst		5.4889E−02	**4.9841E−02**

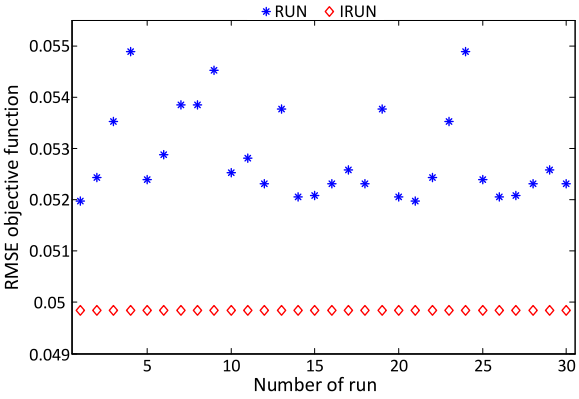


Fig. 13. Scatter plot.

Convergence rates of the standard RUN and proposed IRUN algorithms for the SDM model of the CS6P-220P PV module are displayed in Fig. 14. As can be observed from the convergence curves, both algorithms tend to reach lower RMSE values, however, the proposed IRUN algorithm is capable of reaching the lowest RMSE value and good solution in earlier iterations.

The optimized parameters obtained through the RUN and IRUN algorithms using SDM method were used to estimate the I-V and P-V characteristics of the CS6P-220P PV module cell. Fig. 15 illustrates the close match between the estimated data and the experimental data across the entire voltage range. Here, Fig. 15 (a) displays the I-V characteristics and Fig. 15 (b) shows the P-V characteristics.

We sampled 46 voltage and current values using the measuring devices and variable load from the CS6P-220P PV module depicted in Fig. 5. These sampled values are provided in Table 10. This table also displays the estimated current and absolute current error values optimized by RUN and IRUN algorithms using single-diode model. Other specifications of this module are as follows.

- Test temperature is $30^{\circ}C$.
- Test radiation is 1000 W/m^2.
- Short circuit current is 8.09 A.
- Open circuit voltage is 36.6 V.

As can be seen, the proposed IRUN algorithm reaches MAE and RMSE values of 3.9806E−02 and 4.9841E−02, respectively, outperforming the performance of the standard RUN algorithm. It is worth noting that the adopted dataset obtained from the CS6P-220P PV module has only been used in a work reported in Ref. [15]. In the related work, the squirrel search algorithm applied for estimation of this solar PV module and an RMSE of 0.0710 and a MAE of 0.0556 were attained. As can be observed, the proposed IRUN algorithm significantly outperforms the performance of the reported approach, as well, highlighting its efficacy for the parameter estimation of the real-world practice.

6.2.2. *Double-diode model*

As stated in the previous subsection, we have employed the IRUN algorithm to estimate the unknown parameters of double-diode model associated with CS6P-220P solar PV module, as well. Table 11 reveals the bounds [15] and optimized values of DDM parameters for CS6P-220P PV module. This table also demonstrates the improvements achieved through IRUN methodology, as evidenced by the statistical values of the *RMSE*. It is worth noting that the diode ideality factors (n_1 and n_2), series (R_s) and shunt (R_{sh}) resistance values provided in Table 11 represent the cumulative values for all cells. For individual cells, the diode ideality factor and resistance values are determined by dividing them by the number of cells in series (N_s).

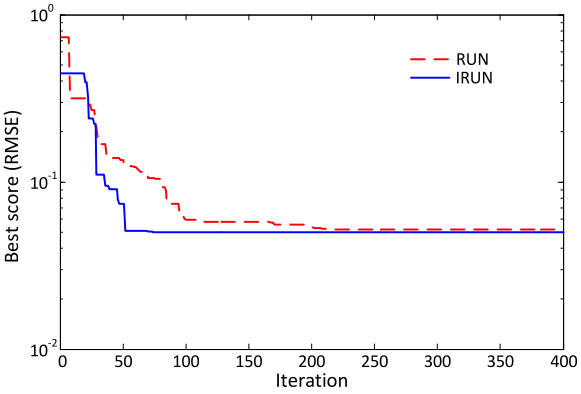


Fig. 14. Convergence rates of RUN and IRUN algorithms for SDM model of CS6P-220P PV module.

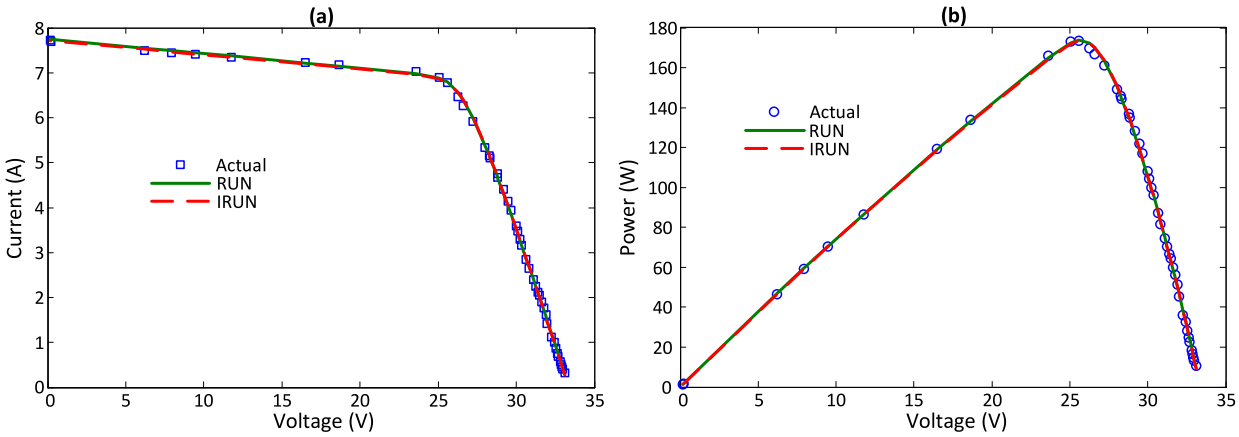


Fig. 15. Characteristics of CS6P-220P PV module using RUN and IRUN algorithms for SDM.

The scatter plot demonstrating the distribution of the RMSE objective function value obtained for each run number of RUN and IRUN algorithms using DDM model of CS6P-220P PV module is displayed in Fig. 16. As can be observed from the illustration in Fig. 16, the proposed IRUN algorithm consistently reaches the lowest RMSE values compared to the standard version of RUN algorithm. Besides, IRUN algorithm has a lower standard deviation indicating its robust nature in terms of reaching good quality solutions. Convergence rates of the standard RUN and proposed IRUN algorithms for the DDM model of the commercially available CS6P-220P PV module are displayed in Fig. 17. As can be observed from the convergence curves, both algorithms tend to reach lower RMSE values, indicating competitive performance of the proposed IRUN algorithm. The optimized parameters obtained through the RUN and IRUN algorithms using DDM method were used to estimate the I-V and P-V characteristics of the CS6P-220P PV module cell. Fig. 18 illustrates the close match between the estimated data and the experimental data across the entire voltage range. Here, Fig. 18 (a) displays the I-V characteristics and Fig. 18 (b) shows the P-V characteristics.

Similar to the SDM case, we performed the analyses for the DDM case as well using the sampled 46 voltage and current values obtained from the CS6P-220P PV module. These sampled values are provided in Table 12. This table also displays the estimated current and absolute current error values optimized by RUN and IRUN algorithms using double-diode model. As can be seen, the proposed IRUN algorithm reaches MAE and RMSE values of 3.9453E−02 and 4.9363E−02, respectively, outperforming the performance of the standard RUN algorithm. As was the case for SDM, the adopted dataset obtained from the CS6P-220P PV module has only been used in a work reported in Ref. [15] for DDM, as well. In the related work, the squirrel search algorithm applied for estimation of this solar PV module and an RMSE of 0.0589 and an MAE of 0.0468 were attained. As can be observed, the proposed IRUN algorithm significantly outperforms the performance of the reported approach, as well, highlighting its efficacy for the parameter estimation of the real-world practice.

6.3. Experimental results for other photovoltaic cell models

6.3.1. Three-diode model

In this section, we present experimental results for the three-diode model (TDM) of the R.T.C. France Solar cell as part of the effort

Table 10
Experimental and estimated current data for CS6P-220P PV module (SDM)

Data no	Voltage (V)	Actual current (A)	Optimized by RUN		Optimized by IRUN	
			Estimated current (A)	Absolute current error (A)	Estimated current (A)	Absolute current error (A)
1	33.1000	0.3230	0.2911	0.0319	0.2763	0.0467
2	32.9700	0.4000	0.4303	0.0303	0.4166	0.0166
3	32.9200	0.4500	0.4838	0.0338	0.4705	0.0205
4	32.8700	0.5030	0.5373	0.0343	0.5244	0.0214
5	32.8000	0.5660	0.6120	0.0460	0.5997	0.0337
6	32.6700	0.6960	0.7507	0.0547	0.7394	0.0434
7	32.6200	0.7630	0.8039	0.0409	0.7931	0.0301
8	32.5200	0.8700	0.9103	0.0403	0.9003	0.0303
9	32.4200	1.0050	1.0165	0.0115	1.0073	0.0023
10	32.2500	1.1170	1.1966	0.0796	1.1889	0.0719
11	31.9800	1.4230	1.4816	0.0586	1.4761	0.0531
12	31.8900	1.6160	1.5763	0.0397	1.5715	0.0445
13	31.7500	1.7750	1.7232	0.0518	1.7195	0.0555
14	31.6200	1.9000	1.8593	0.0407	1.8566	0.0434
15	31.4700	2.0500	2.0158	0.0342	2.0143	0.0357
16	31.3900	2.1230	2.0991	0.0239	2.0982	0.0248
17	31.2500	2.2500	2.2444	0.0056	2.2446	0.0054
18	31.0800	2.4000	2.4202	0.0202	2.4216	0.0216
19	30.8100	2.6450	2.6978	0.0528	2.7011	0.0561
20	30.6400	2.8500	2.8714	0.0214	2.8759	0.0259
21	30.3500	3.1700	3.1653	0.0047	3.1718	0.0018
22	30.2500	3.3000	3.2659	0.0341	3.2731	0.0269
23	30.0900	3.4700	3.4262	0.0438	3.4343	0.0357
24	30.0000	3.6000	3.5158	0.0842	3.5246	0.0754
25	29.6600	3.9500	3.8513	0.0987	3.8620	0.0880
26	29.4700	4.1400	4.0362	0.1038	4.0479	0.0921
27	29.1800	4.4000	4.3146	0.0854	4.3277	0.0723
28	28.8200	4.6800	4.6525	0.0275	4.6669	0.0131
29	28.7800	4.7500	4.6894	0.0606	4.7040	0.0460
30	28.3300	5.1000	5.0955	0.0045	5.1110	0.0110
31	28.2500	5.1600	5.1657	0.0057	5.1812	0.0212
32	28.0000	5.3300	5.3801	0.0501	5.3957	0.0657
33	27.2000	5.9200	6.0051	0.0851	6.0176	0.0976
34	26.5800	6.2700	6.3978	0.1278	6.4037	0.1337
35	26.2400	6.4700	6.5670	0.0970	6.5676	0.0976
36	25.5700	6.7800	6.7930	0.0130	6.7825	0.0025
37	25.0600	6.9000	6.8841	0.0159	6.8675	0.0325
38	23.6000	7.0300	6.9825	0.0475	6.9605	0.0695
39	18.6500	7.1800	7.1465	0.0335	7.1225	0.0575
40	16.4800	7.2300	7.2168	0.0132	7.1921	0.0379
41	11.7500	7.3500	7.3701	0.0201	7.3439	0.0061
42	9.4800	7.4100	7.4437	0.0337	7.4167	0.0067
43	7.9300	7.4500	7.4939	0.0439	7.4664	0.0164
44	6.2000	7.5000	7.5500	0.0500	7.5220	0.0220
45	0.2320	7.7000	7.7434	0.0434	7.7135	0.0135
46	0.1900	7.7200	7.7447	0.0247	7.7148	0.0052
MAE			4.3558E−02		**3.9806E−02**	
RMSE (objective function)			5.1977E−02		**4.9841E−02**	

Table 11
Bounds and optimized values of DDM parameters for CS6P-220P PV module

Parameter	Lower Bound	Upper Bound	Optimized by RUN	Optimized by IRUN
I_{ph} (A)	6	9	7.9371	7.9362
I_{sd1} (A)	1E−35	1E−28	1.0000E−28	1.0000E−28
I_{sd2} (A)	1E−35	1E−28	1.0000E−28	1.0000E−28
R_s (Ω)	0.25	2	0.8509	0.8476
R_{sh} (Ω)	30	60	30.3679	30.3762
n_1	10	25	21.3408	19.4273
n_2	10	25	19.2343	19.4394
RMSE	Average		5.1148E−02	**4.9377E−02**
	Standard Deviation		1.2252E−03	**2.0990E−05**
	Best		4.9896E−02	**4.9363E−02**
	Worst		5.3825E−02	**4.9422E−02**

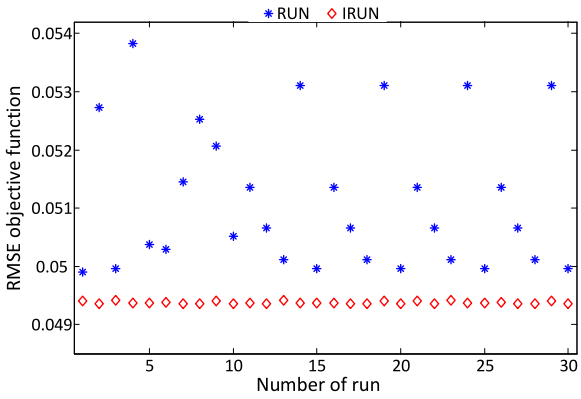


Fig. 16. Scatter plot.

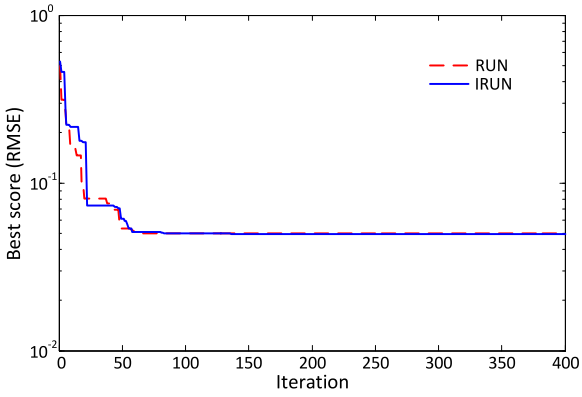


Fig. 17. Convergence rates of RUN and IRUN algorithms for DDM model of CS6P-220P PV module.

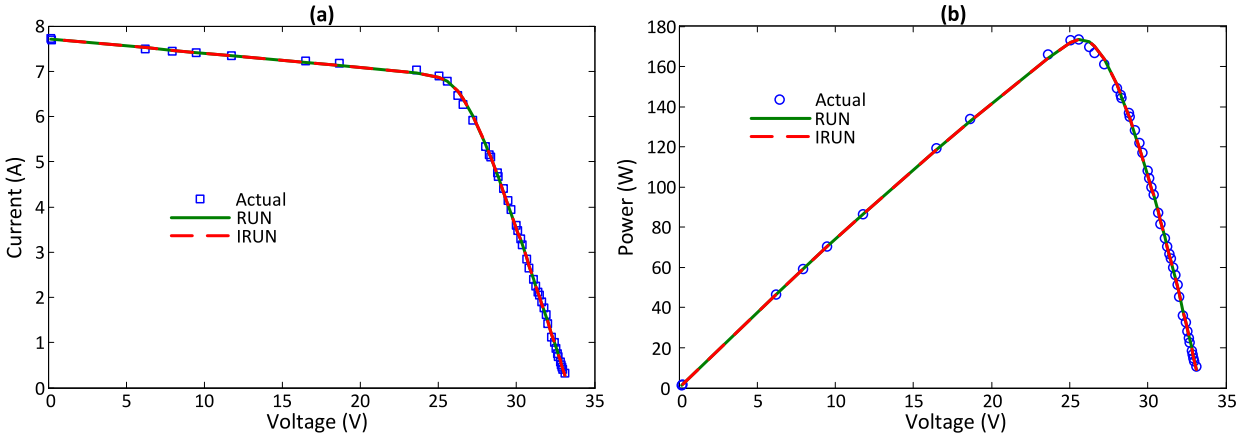


Fig. 18. Characteristics of CS6P-220P PV module using RUN and IRUN algorithms for DDM.

to further demonstrate the efficiency of the proposed IRUN method. The optimized values for the TDM parameters of the R.T.C. France Solar cell, obtained through both the RUN and IRUN methods, are summarized in Table 13. Notably, the RMSE values indicate the superior performance of the proposed IRUN method, showcasing a lower average, standard deviation, best, and worst-case RMSE compared to the RUN method.

Table 14 presents experimental and estimated current data for the RTC France Solar cell, offering a detailed comparison of actual and estimated currents. The MAE and RMSE values for both the RUN and IRUN methods further underscore the efficacy of the

Table 12
Experimental and estimated current data for CS6P-220P PV module (DDM)

Data no	Voltage (V)	Actual current (A)	Optimized by RUN		Optimized by IRUN	
			Estimated current (A)	Absolute current error (A)	Estimated current (A)	Absolute current error (A)
1	33.1000	0.3230	0.2814	0.0416	0.2755	0.0475
2	32.9700	0.4000	0.4214	0.0214	0.4160	0.0160
3	32.9200	0.4500	0.4752	0.0252	0.4699	0.0199
4	32.8700	0.5030	0.5290	0.0260	0.5238	0.0208
5	32.8000	0.5660	0.6042	0.0382	0.5992	0.0332
6	32.6700	0.6960	0.7437	0.0477	0.7391	0.0431
7	32.6200	0.7630	0.7972	0.0342	0.7928	0.0298
8	32.5200	0.8700	0.9042	0.0342	0.9001	0.0301
9	32.4200	1.0050	1.0111	0.0061	1.0072	0.0022
10	32.2500	1.1170	1.1923	0.0753	1.1888	0.0718
11	31.9800	1.4230	1.4789	0.0559	1.4762	0.0532
12	31.8900	1.6160	1.5741	0.0419	1.5717	0.0443
13	31.7500	1.7750	1.7219	0.0531	1.7198	0.0552
14	31.6200	1.9000	1.8588	0.0412	1.8570	0.0430
15	31.4700	2.0500	2.0162	0.0338	2.0148	0.0352
16	31.3900	2.1230	2.0999	0.0231	2.0987	0.0243
17	31.2500	2.2500	2.2460	0.0040	2.2451	0.0049
18	31.0800	2.4000	2.4227	0.0227	2.4223	0.0223
19	30.8100	2.6450	2.7017	0.0567	2.7018	0.0568
20	30.6400	2.8500	2.8762	0.0262	2.8767	0.0267
21	30.3500	3.1700	3.1716	0.0016	3.1726	0.0026
22	30.2500	3.3000	3.2727	0.0273	3.2739	0.0261
23	30.0900	3.4700	3.4337	0.0363	3.4352	0.0348
24	30.0000	3.6000	3.5238	0.0762	3.5254	0.0746
25	29.6600	3.9500	3.8606	0.0894	3.8628	0.0872
26	29.4700	4.1400	4.0463	0.0937	4.0487	0.0913
27	29.1800	4.4000	4.3256	0.0744	4.3284	0.0716
28	28.8200	4.6800	4.6644	0.0156	4.6674	0.0126
29	28.7800	4.7500	4.7014	0.0486	4.7045	0.0455
30	28.3300	5.1000	5.1080	0.0080	5.1111	0.0111
31	28.2500	5.1600	5.1782	0.0182	5.1813	0.0213
32	28.0000	5.3300	5.3925	0.0625	5.3955	0.0655
33	27.2000	5.9200	6.0144	0.0944	6.0164	0.0964
34	26.5800	6.2700	6.4012	0.1312	6.4019	0.1319
35	26.2400	6.4700	6.5658	0.0958	6.5657	0.0957
36	25.5700	6.7800	6.7821	0.0021	6.7813	0.0013
37	25.0600	6.9000	6.8680	0.0320	6.8673	0.0327
38	23.6000	7.0300	6.9616	0.0684	6.9615	0.0685
39	18.6500	7.1800	7.1234	0.0566	7.1234	0.0566
40	16.4800	7.2300	7.1929	0.0371	7.1929	0.0371
41	11.7500	7.3500	7.3444	0.0056	7.3444	0.0056
42	9.4800	7.4100	7.4171	0.0071	7.4171	0.0071
43	7.9300	7.4500	7.4668	0.0168	7.4667	0.0167
44	6.2000	7.5000	7.5222	0.0222	7.5221	0.0221
45	0.2320	7.7000	7.7134	0.0134	7.7133	0.0133
46	0.1900	7.7200	7.7147	0.0053	7.7146	0.0054
MAE			4.0181E−02		**3.9453E−02**	
RMSE (objective function)			4.9896E−02		**4.9363E−02**	

proposed IRUN method in achieving a lower error in current estimation.

Table 15 provides a comparative analysis of parameter estimation results for the TDM of the RTC France Solar cell using the IRUN method, the proposed RUN method, and other existing methods. The table clearly demonstrates that the IRUN method yields optimized parameter values with a lower RMSE compared to other methods, emphasizing its superior performance in accurately estimating the TDM parameters.

6.3.2. STM6-40/36 PV module model

In this section, we analyze the efficiency of the proposed IRUN in parameter estimation for the STM6-40/36 PV module model. Table 16 outlines the bounds and optimized values of PV module parameters obtained through both the RUN and IRUN methods. Remarkably, the IRUN method achieves an average RMSE value (1.7219E−03) significantly lower than that of the RUN method (1.7230E−03), emphasizing its superior accuracy in parameter estimation.

In Table 17, we observe a detailed comparison of experimental and estimated current data for the STM6-40/36 PV module. For example, at data point 1, both IRUN and RUN methods exhibit minor absolute current errors (0.0005 and 0.0004, respectively). At data point 13, IRUN shows a slightly higher absolute current error (0.0017) compared to RUN (0.0015). The MAE values underscore the

Table 13
Bounds and optimized values of TDM parameters for RTC France solar cell

Parameter	Lower bound	Upper Bound	Optimized by RUN	Optimized by IRUN
I_{ph} (A)	0	1	0.7608	0.7608
I_{sd1} (A)	0	1E−06	3.2209E−07	6.0814E−07
I_{sd2} (A)	0	1E−06	5.2528E−08	8.9971E−07
I_{sd3} (A)	0	1E−06	3.5331E−08	9.4215E−08
R_s (Ω)	0	0.5	0.0368	0.0377
R_{sh} (Ω)	0	100	53.3614	57.1237
n_1	1	2	1.5421	1.9282
n_2	1	2	1.3872	1.9201
n_3	1	2	2.0000	1.3814
RMSE	Average		7.7151E−04	**7.4617E−04**
	Standard Deviation		**2.6324E−06**	5.3000E−06
	Best		7.6555E−04	**7.3668E−04**
	Worst		7.7501E−04	**7.5357E−04**

Table 14
Experimental and estimated current data for R.T.C France solar cell (TDM)

Data no	Voltage (V)	Actual current (A)	Optimized by RUN		Optimized by IRUN	
			Estimated current (A)	Absolute current error (A)	Estimated current (A)	Absolute current error (A)
1	−0.2057	0.7640	0.7641	0.0001	0.7639	0.0001
2	−0.1291	0.7620	0.7627	0.0007	0.7626	0.0006
3	−0.0588	0.7605	0.7614	0.0009	0.7613	0.0008
4	0.0057	0.7605	0.7602	0.0003	0.7602	0.0003
5	0.0646	0.7600	0.7591	0.0009	0.7592	0.0008
6	0.1185	0.7590	0.7581	0.0009	0.7582	0.0008
7	0.1678	0.7570	0.7571	0.0001	0.7573	0.0003
8	0.2132	0.7570	0.7561	0.0009	0.7563	0.0007
9	0.2545	0.7555	0.7551	0.0004	0.7552	0.0003
10	0.2924	0.7540	0.7536	0.0004	0.7537	0.0003
11	0.3269	0.7505	0.7513	0.0008	0.7513	0.0008
12	0.3585	0.7465	0.7473	0.0008	0.7471	0.0006
13	0.3873	0.7385	0.7400	0.0015	0.7398	0.0013
14	0.4137	0.7280	0.7273	0.0007	0.7271	0.0009
15	0.4373	0.7065	0.7069	0.0004	0.7067	0.0002
16	0.4590	0.6755	0.6753	0.0002	0.6753	0.0002
17	0.4784	0.6320	0.6310	0.0010	0.6311	0.0009
18	0.4960	0.5730	0.5722	0.0008	0.5724	0.0006
19	0.5119	0.4990	0.4996	0.0006	0.4998	0.0008
20	0.5265	0.4130	0.4135	0.0005	0.4136	0.0006
21	0.5398	0.3165	0.3172	0.0007	0.3172	0.0007
22	0.5521	0.2120	0.2120	0.0000	0.2119	0.0001
23	0.5633	0.1035	0.1026	0.0009	0.1024	0.0011
24	0.5736	−0.0100	−0.0093	0.0007	−0.0095	0.0005
25	0.5833	−0.1230	−0.1244	0.0014	−0.1244	0.0014
26	0.5900	−0.2100	−0.2091	0.0009	−0.2089	0.0011
MAE			6.7518E−04		**6.5000E−04**	
RMSE (objective function)			7.6555E−04		**7.3668E−04**	

Table 15
The result of parameter estimation by IRUN and other methods on TDM of R.T. France solar cell

Method	I_{ph} (A)	I_{sd1} (A)	I_{sd2} (A)	I_{sd3} (A)	R_s (Ω)	R_{sh} (Ω)	n_1	n_2	n_3	RMSE
IRUN (proposed)	0.7608	6.0814E−07	8.9971E−07	9.4215E−08	0.0377	57.1237	1.9282	1.9201	1.3814	**7.3668E−04**
RUN (proposed)	0.7608	3.2209E−07	5.2528E−08	3.5331E−08	0.0368	53.3614	1.5421	1.3872	2.0000	7.6555E−04
MRFO [29]	0.7607	2.6318E−07	2.3678E−07	2.5070E−07	0.0367	55.0167	1.9131	1.4551	1.9965	7.6083E−04
CNGPS [48]	0.7608	2.2842E−07	7.2633E−07	4.9184E−07	0.0369	55.3988	1.4519	2	1.9993	9.8249E−04
NGO [48]	0.7608	3.0707E−07	5.4239E−07	2.1457E−07	0.0368	55.7599	2	2	1.4467	9.8256E−04
SDGBO [53]	0.7608	2.2842E−07	7.2633E−07	4.9184E−15	0.0369	55.3988	1.4519	2	1.9993	9.8249E−04
SCA [53]	0.7656	1.7471E−07	9.5700E−09	3.6900E−07	0.0366	36.6203	1.4254	1.4579	2.0000	8.9010E−03

Table 16
Bounds and optimized values of PV module parameters

Parameter	Lower bound	Upper Bound	Optimized by RUN	Optimized by IRUN
I_{ph} (A)	0	2	1.6638	1.6639
I_{sd} (A)	0	5E−05	1.7774E−06	1.7412E−06
R_s (Ω)	0	0.36	0.1516	0.1536
R_{sh} (Ω)	0	1000	578.9778	573.5339
n	1	60	54.8182	54.7369
RMSE	Average		1.7230E−03	**1.7219E−03**
	Standard Deviaiton		2.5875E−07	**1.1027E−18**
	Best		1.7228E−03	**1.7219E−03**
	Worst		1.7237E−03	**1.7219E−03**

Table 17
Experimental and estimated current data for PV module model of STM6-40/36 module

Data no	Voltage (V)	Actual current (A)	Optimized by RUN		Optimized by IRUN	
			Estimated current (A)	Absolute current error (A)	Estimated current (A)	Absolute current error (A)
1	0	1.6630	1.6634	0.0004	1.6635	0.0005
2	0.1180	1.6630	1.6632	0.0002	1.6633	0.0003
3	2.2370	1.6610	1.6595	0.0015	1.6596	0.0014
4	5.4340	1.6530	1.6539	0.0009	1.6539	0.0009
5	7.2600	1.6500	1.6506	0.0006	1.6506	0.0006
6	9.6800	1.6450	1.6455	0.0005	1.6454	0.0004
7	11.5900	1.6400	1.6393	0.0007	1.6392	0.0008
8	12.6000	1.6360	1.6338	0.0022	1.6337	0.0023
9	13.3700	1.6290	1.6273	0.0017	1.6273	0.0017
10	14.0900	1.6190	1.6184	0.0006	1.6183	0.0007
11	14.8800	1.5970	1.6031	0.0061	1.6031	0.0061
12	15.5900	1.5810	1.5816	0.0006	1.5816	0.0006
13	16.4000	1.5420	1.5423	0.0003	1.5423	0.0003
14	16.7100	1.5240	1.5212	0.0028	1.5212	0.0028
15	16.9800	1.5000	1.4991	0.0009	1.4992	0.0008
16	17.1300	1.4850	1.4852	0.0002	1.4853	0.0003
17	17.3200	1.4650	1.4656	0.0006	1.4656	0.0006
18	17.9100	1.3880	1.3875	0.0005	1.3876	0.0004
19	19.0800	1.1180	1.1184	0.0004	1.1184	0.0004
20	21.0200	0	−0.0001	0.0001	0	0.0000
MAE			**1.0783E−03**		1.0895E−03	
RMSE (objective function)			1.7228E−03		**1.7219E−03**	

Table 18
The result of parameter estimation by IRUN and other methods on PV module of STM6-40/36 PV module

Method	I_{ph} (A)	I_{sd} (A)	R_s (Ω)	R_{sh} (Ω)	n	RMSE
IRUN (proposed)	1.6639	1.7412E−06	0.0043	15.9315	1.5205	**1.7219E−03**
RUN (proposed)	1.6638	1.7774E−06	0.0042	16.0827	1.5227	1.7228E−03
ELADE [45]	1.6639	1.7387E−06	0.0043	15.9283	1.5203	1.7298E−03
L-SHADE [45]	1.6639	1.7387E−06	0.0043	15.9284	1.5203	1.7298E−03
IQSODE [47]	1.6639	1.7387E−06	0.0043	15.9283	1.5203	1.7298E−03
BES [74]	1.6639	1.7387E−06	0.0043	15.9283	1.5203	1.7298E−03
GOTLGO [74]	1.6639	1.7387E−06	0.0043	15.9283	1.5203	1.7298E−03

*Note: The reported diode ideality factor along with series and shunt resistances are per cell.

consistency of both methods, with IRUN showcasing a slightly higher absolute error. Besides, the IRUN achieves the lower RMSE value showcasing its efficiency.

Table 18 offers a comparative analysis of parameter estimation results for the PV module of STM6-40/36, demonstrating the efficacy of the IRUN method. RMSE value by IRUN (1.7219E−03) is noticeably lower than that obtained by other methods, including RUN (1.7228E−03). Optimized parameter values obtained by IRUN, such as diode saturation current and shunt resistance, contribute to this superior accuracy.

7. Conclusion

In this research, we have demonstrated power of the IRUN algorithm to estimate the parameters in PV systems. The proposed approach significantly improves the effectiveness and precision of parameter estimation. Our study revolves around CEC 2020 benchmark functions and two distinct solar PV equivalent circuit models, SDM and DDM, both of which have been meticulously evaluated and dissected through two captivating case studies. Besides, additional TDM and PV module models were also used as additional test beds for performance confirmation. In the first case study, our focus centers on modeling a single solar cell, utilizing the standardized dataset derived from a commercially renowned R.T.C. France silicon solar cell. Through the sheer power of IRUN, we have successfully unraveled the optimal parameter values for both the SDM and DDM of this cell. To highlight the profound impact of our proposed approach, we have engaged in a rigorous comparison with several state-of-the-art schemes published recently in the field. The results of this extensive analysis show that the IRUN algorithm boasts the most remarkable RMSE values for both the SDM and DDM cases. Its precision underscores its effectiveness in parameter estimation tasks. In the second case study, we venture into the realm of empirical experimentation, conducting tests on a CS6P-220P PV module deployed at the Engineering Faculty of Düzce university in Turkey. Armed with the acquired experimental dataset, IRUN algorithm once again takes the center stage, expertly determining the optimal values for the SDM and DDM parameters specific to this module. The simulated I-V and P-V characteristics of our data align with the experimental results, affirming the remarkable accuracy of our approach across the entire voltage range. The analyses on TDM of R.T.C. France silicon solar cell and PV model of STM6-40/36 PV module further verified the efficacy of the IRUN from a wider perspective. In light of these findings, the IRUN algorithm demonstrates considerable potential and strong performance in solar PV parameter estimation.

CRediT authorship contribution statement

Serdar Ekinci: Writing – review & editing, Visualization, Software, Methodology, Investigation, Formal analysis, Data curation, Conceptualization. **Rizk M. Rizk-Allah:** Writing – original draft, Visualization, Validation, Software, Data curation, Conceptualization. **Davut Izci:** Writing – original draft, Validation, Methodology, Investigation, Formal analysis, Data curation, Conceptualization. **Emre Çelik:** Writing – review & editing, Validation, Supervision, Software.

Data availability statement

All generated or analyzed data during this study are included in the paper.

Declaration of competing interest

The authors declare that they have no known competing financial interests or personal relationships that could have appeared to influence the work reported in this paper.

References

[1] J. Zhang, D. Kong, Y. He, X. Fu, X. Zhao, G. Yao, F. Teng, Y. Qin, Bi-layer energy optimal scheduling of regional integrated energy system considering variable correlations, Int. J. Electr. Power Energy Syst. 148 (2023) 108840, https://doi.org/10.1016/j.ijepes.2022.108840.
[2] R.M. Rizk-Allah, A. Ella Hassanien, Locomotion-based hybrid salp swarm algorithm for parameter estimation of fuzzy representation-based photovoltaic modules, Journal of Modern Power Systems and Clean Energy 9 (2021) 384–394, https://doi.org/10.35833/MPCE.2019.000028.
[3] S. Ekinci, Ö. Can, M.Ş. Ayas, D. Izci, M. Salman, M. Rashdan, Automatic generation control of a hybrid PV-reheat thermal power system using RIME algorithm, IEEE Access 12 (2024) 26919–26930, https://doi.org/10.1109/ACCESS.2024.3367011.
[4] R.M. Rizk-Allah, A.A. El-Fergany, Emended heap-based optimizer for characterizing performance of industrial solar generating units using triple-diode model, Energy 237 (2021) 121561, https://doi.org/10.1016/j.energy.2021.121561.
[5] S. Ekinci, D. Izci, A.G. Hussien, Comparative analysis of the hybrid gazelle-Nelder–Mead algorithm for parameter extraction and optimization of solar photovoltaic systems, IET Renew. Power Gener. (2024), https://doi.org/10.1049/rpg2.12974.
[6] M. Premkumar, P. Jangir, R. Sowmya, Parameter extraction of three-diode solar photovoltaic model using a new metaheuristic resistance–capacitance optimization algorithm and improved Newton–Raphson method, J. Comput. Electron. (2022), https://doi.org/10.1007/s10825-022-01987-6.
[7] M. Premkumar, N. Shankar, R. Sowmya, P. Jangir, C. Kumar, L. Abualigah, B. Derebew, A reliable optimization framework for parameter identification of single-diode solar photovoltaic model using weighted velocity-guided grey wolf optimization algorithm and Lambert-W function, IET Renew. Power Gener. (2023), https://doi.org/10.1049/rpg2.12792.
[8] M. Premkumar, P. Jangir, C. Ramakrishnan, C. Kumar, R. Sowmya, S. Deb, N.M. Kumar, An enhanced Gradient-based Optimizer for parameter estimation of various solar photovoltaic models, Energy Rep. 8 (2022) 15249–15285, https://doi.org/10.1016/j.egyr.2022.11.092.
[9] M. Premkumar, P. Jangir, C. Kumar, S.D.T. Sundarsingh Jebaseelan, H.H. Alhelou, R. Madurai Elavarasan, H. Chen, Constraint estimation in three-diode solar photovoltaic model using Gaussian and Cauchy mutation-based hunger games search optimizer and enhanced Newton–Raphson method, IET Renew. Power Gener. 16 (2022) 1733–1772, https://doi.org/10.1049/rpg2.12475.
[10] M. Premkumar, P. Jangir, R. Sowmya, R.M. Elavarasan, B.S. Kumar, Enhanced chaotic JAYA algorithm for parameter estimation of photovoltaic cell/modules, ISA Trans. 116 (2021) 139–166, https://doi.org/10.1016/j.isatra.2021.01.045.
[11] M. Premkumar, P. Jangir, R.M. Elavarasan, R. Sowmya, Opposition decided gradient-based optimizer with balance analysis and diversity maintenance for parameter identification of solar photovoltaic models, J Ambient Intell Humaniz Comput 14 (2023) 7109–7131, https://doi.org/10.1007/s12652-021-03564-4.
[12] M. Premkumar, P. Jangir, C. Ramakrishnan, G. Nalinipriya, H.H. Alhelou, B.S. Kumar, Identification of solar photovoltaic model parameters using an improved gradient-based optimization algorithm with chaotic drifts, IEEE Access 9 (2021) 62347–62379, https://doi.org/10.1109/ACCESS.2021.3073821.
[13] M. Premkumar, R. Sowmya, S. Umashankar, P. Jangir, Extraction of uncertain parameters of single-diode photovoltaic module using hybrid particle swarm optimization and grey wolf optimization algorithm, Mater Today Proc 46 (2021) 5315–5321, https://doi.org/10.1016/j.matpr.2020.08.784.

[14] M. Premkumar, R. Sowmya, P. Jangir, J.S.V. Siva Kumar, A new and reliable objective functions for extracting the unknown parameters of solar photovoltaic cell using political optimizer algorithm, in: 2020 International Conference on Data Analytics for Business and Industry: Way towards a Sustainable Economy (ICDABI), IEEE, 2020, pp. 1–6, https://doi.org/10.1109/ICDABI51230.2020.9325627.

[15] D. Maden, E. Çelik, E.H. Houssein, G. Sharma, Squirrel search algorithm applied to effective estimation of solar PV model parameters: a real-world practice, Neural Comput. Appl. 35 (2023) 13529–13546, https://doi.org/10.1007/s00521-023-08451-x.

[16] R. Ben Messaoud, Extraction of uncertain parameters of single-diode model of a photovoltaic panel using simulated annealing optimization, Energy Rep. 6 (2020) 350–357, https://doi.org/10.1016/j.egyr.2020.01.016.

[17] H. Saleem, S. Karmalkar, An analytical method to extract the physical parameters of a solar cell from four points on the illuminated $J{-}V$ curve, IEEE Electron. Device Lett. 30 (2009) 349–352, https://doi.org/10.1109/LED.2009.2013882.

[18] R.M. Rizk-Allah, M.I. Abdelwanis, R.A. El-Sehiemy, A.S. Abd-Elrazek, An interior search algorithm based on chaotic and crossover strategies for parameter extraction of polyphase induction machines, Neural Comput. Appl. 35 (2023) 6647–6664, https://doi.org/10.1007/s00521-022-08055-x.

[19] X. Chen, H. Yue, K. Yu, Perturbed stochastic fractal search for solar PV parameter estimation, Energy 189 (2019) 116247, https://doi.org/10.1016/j.energy.2019.116247.

[20] A.A.K. Ismaeel, E.H. Houssein, D. Oliva, M. Said, Gradient-based optimizer for parameter extraction in photovoltaic models, IEEE Access 9 (2021) 13403–13416, https://doi.org/10.1109/ACCESS.2021.3052153.

[21] M.A. Khelifa, B. Lekouaghet, A. Boukabou, Symmetric chaotic gradient-based optimizer algorithm for efficient estimation of PV parameters, Optik 259 (2022) 168873, https://doi.org/10.1016/j.ijleo.2022.168873.

[22] M. Qaraad, S. Amjad, N.K. Hussein, M. Badawy, S. Mirjalili, M.A. Elhosseini, Photovoltaic parameter estimation using improved moth flame algorithms with local escape operators, Comput. Electr. Eng. 106 (2023) 108603, https://doi.org/10.1016/j.compeleceng.2023.108603.

[23] A.M. Eltamaly, Musical chairs algorithm for parameters estimation of PV cells, Sol. Energy 241 (2022) 601–620, https://doi.org/10.1016/j.solener.2022.06.043.

[24] H.A. Ramadan, B. Khan, A.A.Z. Diab, Accurate parameters estimation of three diode model of photovoltaic modules using hunter–prey and wild horse optimizers, IEEE Access 10 (2022) 87435–87453, https://doi.org/10.1109/ACCESS.2022.3199001.

[25] J.J. Montano, L.F. Grisales Norena, A.F. Tobon, D. Gonzalez Montoya, Estimation of the parameters of the mathematical model of an equivalent diode of a photovoltaic panel using a continuous genetic algorithm, IEEE Latin America Transactions 20 (2022) 616–623, https://doi.org/10.1109/TLA.2022.9675467.

[26] M. Yaghoubi, M. Eslami, M. Noroozi, H. Mohammadi, O. Kamari, S. Palani, Modified salp swarm optimization for parameter estimation of solar PV models, IEEE Access 10 (2022) 110181–110194, https://doi.org/10.1109/ACCESS.2022.3213746.

[27] Jovanović Ćalasan, Rubežić, mujović, đukanović, estimation of single-diode and two-diode solar cell parameters by using a chaotic optimization approach, Energies 12 (2019) 4209, https://doi.org/10.3390/en12214209.

[28] R.M. Rizk-Allah, A.A. El-Fergany, Conscious neighborhood scheme-based Laplacian barnacles mating algorithm for parameters optimization of photovoltaic single- and double-diode models, Energy Convers. Manag. 226 (2020) 113522, https://doi.org/10.1016/j.enconman.2020.113522.

[29] E.H. Houssein, G.N. Zaki, A.A.Z. Diab, E.M.G. Younis, An efficient Manta Ray Foraging Optimization algorithm for parameter extraction of three-diode photovoltaic model, Comput. Electr. Eng. 94 (2021) 107304, https://doi.org/10.1016/j.compeleceng.2021.107304.

[30] M. Abdel-Basset, R. Mohamed, R.K. Chakrabortty, M.J. Ryan, A. El-Fergany, An improved artificial jellyfish search optimizer for parameter identification of photovoltaic models, Energies 14 (2021) 1867, https://doi.org/10.3390/en14071867.

[31] A. Singh, A. Sharma, S. Rajput, A.K. Mondal, A. Bose, M. Ram, Parameter extraction of solar module using the sooty tern optimization algorithm, Electronics (Basel) 11 (2022) 564, https://doi.org/10.3390/electronics11040564.

[32] TummalaS.L. V Ayyarao, P.P. Kumar, Parameter estimation of solar PV models with a new proposed war strategy optimization algorithm, Int. J. Energy Res. 46 (2022) 7215–7238, https://doi.org/10.1002/er.7629.

[33] S. Duman, H.T. Kahraman, Y. Sonmez, U. Guvenc, M. Kati, S. Aras, A powerful meta-heuristic search algorithm for solving global optimization and real-world solar photovoltaic parameter estimation problems, Eng. Appl. Artif. Intell. 111 (2022) 104763, https://doi.org/10.1016/j.engappai.2022.104763.

[34] Q. Bo, W. Cheng, M. Khishe, M. Mohammadi, A.H. Mohammed, Solar photovoltaic model parameter identification using robust niching chimp optimization, Sol. Energy 239 (2022) 179–197, https://doi.org/10.1016/j.solener.2022.04.056.

[35] I. Ahmadianfar, A.A. Heidari, A.H. Gandomi, X. Chu, H. Chen, RUN beyond the metaphor: an efficient optimization algorithm based on Runge Kutta method, Expert Syst. Appl. 181 (2021) 115079, https://doi.org/10.1016/j.eswa.2021.115079.

[36] J.O. Agushaka, A.E. Ezugwu, L. Abualigah, Dwarf mongoose optimization algorithm, Comput. Methods Appl. Mech. Eng. 391 (2022) 114570, https://doi.org/10.1016/j.cma.2022.114570.

[37] S. Mirjalili, A.H. Gandomi, S.Z. Mirjalili, S. Saremi, H. Faris, S.M. Mirjalili, Salp Swarm Algorithm: a bio-inspired optimizer for engineering design problems, Adv. Eng. Software 114 (2017) 163–191, https://doi.org/10.1016/j.advengsoft.2017.07.002.

[38] S. Mirjalili, S.M. Mirjalili, A. Lewis, Grey wolf optimizer, Adv. Eng. Software 69 (2014) 46–61, https://doi.org/10.1016/j.advengsoft.2013.12.007.

[39] A.E. Ezugwu, J.O. Agushaka, L. Abualigah, S. Mirjalili, A.H. Gandomi, Prairie dog optimization algorithm, Neural Comput. Appl. 34 (2022) 20017–20065, https://doi.org/10.1007/s00521-022-07530-9.

[40] D. Simon, Biogeography-based optimization, IEEE Trans. Evol. Comput. 12 (2008) 702–713, https://doi.org/10.1109/TEVC.2008.919004.

[41] J. Kennedy, R. Eberhart, Particle swarm optimization, in: Proceedings of ICNN'95-International Conference on Neural Networks, IEEE, 1995, pp. 1942–1948.

[42] J.O. Agushaka, A.E. Ezugwu, L. Abualigah, Gazelle optimization algorithm: a novel nature-inspired metaheuristic optimizer, Neural Comput. Appl. (2022), https://doi.org/10.1007/s00521-022-07854-6.

[43] R. Storn, K. Price, Differential evolution - a simple and efficient heuristic for global optimization over continuous spaces, J. Global Optim. 11 (1997) 341–359, https://doi.org/10.1023/A:1008202821328.

[44] S. Mirjalili, SCA: a Sine Cosine Algorithm for solving optimization problems, Knowl Based Syst 96 (2016) 120–133, https://doi.org/10.1016/j.knosys.2015.12.022.

[45] Z. Gu, G. Xiong, X. Fu, A.W. Mohamed, M.A. Al-Betar, H. Chen, J. Chen, Extracting accurate parameters of photovoltaic cell models via elite learning adaptive differential evolution, Energy Convers. Manag. 285 (2023) 116994, https://doi.org/10.1016/j.enconman.2023.116994.

[46] Y. Lu, S. Liang, H. Ouyang, S. Li, G. Wang, Hybrid multi-group stochastic cooperative particle swarm optimization algorithm and its application to the photovoltaic parameter identification problem, Energy Rep. 9 (2023) 4654–4681, https://doi.org/10.1016/j.egyr.2023.03.105.

[47] A.A. Abd El-Mageed, A.A. Abohany, H.M.H. Saad, K.M. Sallam, Parameter extraction of solar photovoltaic models using queuing search optimization and differential evolution, Appl. Soft Comput. 134 (2023) 110032, https://doi.org/10.1016/j.asoc.2023.110032.

[48] H. Satria, R.B.Y. Syah, M.L. Nehdi, M.K. Almustafa, A.O.I. Adam, Parameters identification of solar PV using hybrid chaotic northern goshawk and pattern search, Sustainability 15 (2023) 5027, https://doi.org/10.3390/su15065027.

[49] C. Yang, C. Su, H. Hu, M. Habibi, H. Safarpour, M. Amine Khadimallah, Performance optimization of photovoltaic and solar cells via a hybrid and efficient chimp algorithm, Sol. Energy 253 (2023) 343–359, https://doi.org/10.1016/j.solener.2023.02.036.

[50] T. Taleshian, N. A.R, M. Malekzadeh, J. Sadati, Parameters identification of photovoltaic solar cells using FIPSO-SQP algorithm, Optik 283 (2023) 170900, https://doi.org/10.1016/j.ijleo.2023.170900.

[51] D. Izci, S. Ekinci, S. Dal, N. Sezgin, Parameter estimation of solar cells via weighted mean of vectors algorithm, in: 2022 Global Energy Conference (GEC), IEEE, 2022, pp. 312–316, https://doi.org/10.1109/GEC55014.2022.9986943.

[52] Y. Kharchouf, R. Herbazi, A. Chahboun, Parameter's extraction of solar photovoltaic models using an improved differential evolution algorithm, Energy Convers. Manag. 251 (2022) 114972, https://doi.org/10.1016/j.enconman.2021.114972.

[53] S. Yu, Z. Chen, A.A. Heidari, W. Zhou, H. Chen, L. Xiao, Parameter identification of photovoltaic models using a sine cosine differential gradient based optimizer, IET Renew. Power Gener. 16 (2022) 1535–1561, https://doi.org/10.1049/rpg2.12451.

[54] B. Xu, A.A. Heidari, F. Kuang, S. Zhang, H. Chen, Z. Cai, Quantum nelder-mead hunger games search for optimizing photovoltaic solar cells, Int. J. Energy Res. 46 (2022) 12417–12466, https://doi.org/10.1002/er.8011.
[55] B. Arandian, M. Eslami, S.Abd Khalid, B. Khan, U.U. Sheikh, E. Akbari, A.H. Mohammed, An effective optimization algorithm for parameters identification of photovoltaic models, IEEE Access 10 (2022) 34069–34084, https://doi.org/10.1109/ACCESS.2022.3161467.
[56] A. Ramadan, S. Kamel, A. Korashy, A. Almalaq, J.L. Domínguez-García, An enhanced Harris Hawk optimization algorithm for parameter estimation of single, double and triple diode photovoltaic models, Soft Comput. 26 (2022) 7233–7257, https://doi.org/10.1007/s00500-022-07109-5.
[57] I. Ahmadianfar, W. Gong, A.A. Heidari, N.A. Golilarz, A. Samadi-Koucheksaraee, H. Chen, Gradient-based optimization with ranking mechanisms for parameter identification of photovoltaic systems, Energy Rep. 7 (2021) 3979–3997, https://doi.org/10.1016/j.egyr.2021.06.064.
[58] H. Rezk, T.S. Babu, M. Al-Dhaifallah, H.A. Ziedan, A robust parameter estimation approach based on stochastic fractal search optimization algorithm applied to solar PV parameters, Energy Rep. 7 (2021) 620–640, https://doi.org/10.1016/j.egyr.2021.01.024.
[59] A.A.Z. Diab, H.M. Sultan, T.D. Do, O.M. Kamel, M.A. Mossa, Coyote optimization algorithm for parameters estimation of various models of solar cells and PV modules, IEEE Access 8 (2020) 111102–111140, https://doi.org/10.1109/ACCESS.2020.3000770.
[60] N. Pourmousa, S.M. Ebrahimi, M. Malekzadeh, M. Alizadeh, Parameter estimation of photovoltaic cells using improved Lozi map based chaotic optimization Algorithm, Sol. Energy 180 (2019) 180–191, https://doi.org/10.1016/j.solener.2019.01.026.
[61] H. Sheng, C. Li, H. Wang, Z. Yan, Y. Xiong, Z. Cao, Q. Kuang, Parameters extraction of photovoltaic models using an improved moth-flame optimization, Energies 12 (2019) 3527, https://doi.org/10.3390/en12183527.
[62] A.M. Beigi, A. Maroosi, Parameter identification for solar cells and module using a hybrid firefly and pattern search algorithms, Sol. Energy 171 (2018) 435–446, https://doi.org/10.1016/j.solener.2018.06.092.
[63] K. Yu, J.J. Liang, B.Y. Qu, X. Chen, H. Wang, Parameters identification of photovoltaic models using an improved JAYA optimization algorithm, Energy Convers. Manag. 150 (2017) 742–753, https://doi.org/10.1016/j.enconman.2017.08.063.
[64] D. Oliva, E. Cuevas, G. Pajares, Parameter identification of solar cells using artificial bee colony optimization, Energy 72 (2014) 93–102, https://doi.org/10.1016/j.energy.2014.05.011.
[65] D. Izci, S. Ekinci, S. Mirjalili, Optimal PID plus second-order derivative controller design for AVR system using a modified Runge Kutta optimizer and Bode's ideal reference model, Int J Dyn Control 11 (2023) 1247–1264, https://doi.org/10.1007/s40435-022-01046-9.
[66] D. Izci, S. Ekinci, An improved RUN optimizer based real PID plus second-order derivative controller design as a novel method to enhance transient response and robustness of an automatic voltage regulator, E-Prime - advances in Electrical Engineering, Electronics and Energy 2 (2022) 100071, https://doi.org/10.1016/j.prime.2022.100071.
[67] R.M. Rizk-Allah, A.E. Hassanien, A comprehensive survey on the sine–cosine optimization algorithm, Artif. Intell. Rev. 56 (2023) 4801–4858, https://doi.org/10.1007/s10462-022-10277-3.
[68] W. Guo, Y. Wang, F. Dai, P. Xu, Improved sine cosine algorithm combined with optimal neighborhood and quadratic interpolation strategy, Eng. Appl. Artif. Intell. 94 (2020) 103779, https://doi.org/10.1016/j.engappai.2020.103779.
[69] X. Weng, A.A. Heidari, G. Liang, H. Chen, X. Ma, M. Mafarja, H. Turabieh, Laplacian Nelder-Mead spherical evolution for parameter estimation of photovoltaic models, Energy Convers. Manag. 243 (2021) 114223, https://doi.org/10.1016/j.enconman.2021.114223.
[70] R.M. Rizk-Allah, A.E. Hassanien, D. Song, Chaos-opposition-enhanced slime mould algorithm for minimizing the cost of energy for the wind turbines on high-altitude sites, ISA Trans. 121 (2022) 191–205, https://doi.org/10.1016/j.isatra.2021.04.011.
[71] O. Tarkhaneh, H. Shen, Training of feedforward neural networks for data classification using hybrid particle swarm optimization, Mantegna Lévy flight and neighborhood search, Heliyon 5 (2019) e01275, https://doi.org/10.1016/j.heliyon.2019.e01275.
[72] T. Easwarakhanthan, J. Bottin, I. Bouhouch, C. Boutrit, Nonlinear minimization algorithm for determining the solar cell parameters with microcomputers, Int. J. Sol. Energy 4 (1986) 1–12, https://doi.org/10.1080/01425918608909835.
[73] T.S.L.V. Ayyarao, Parameter estimation of solar PV models with quantum-based avian navigation optimizer and Newton–Raphson method, J. Comput. Electron. 21 (2022) 1338–1356, https://doi.org/10.1007/s10825-022-01931-8.
[74] N.F. Nicaire, P.N. Steve, N.E. Salome, A.O. Grégroire, Parameter estimation of the photovoltaic system using bald eagle search (BES) algorithm, Int. J. Photoenergy 2021 (2021) 1–20, https://doi.org/10.1155/2021/4343203.